8-2023

Femoral Osteohistology in American Alligators (Alligator mississippiensis) Reveals High Variation in Growth and Facilitates Interpretation of an Early Pliocene Alligator

Davis Gunnin
East Tennessee State University

Recommended Citation

Gunnin, Davis, "Femoral Osteohistology in American Alligators (Alligator mississippiensis) Reveals High Variation in Growth and Facilitates Interpretation of an Early Pliocene Alligator" (2023). *Electronic Theses and Dissertations.* Paper 4263. https://dc.etsu.edu/etd/4263

Femoral Osteohistology in American Alligators (*Alligator mississippiensis*) Reveals High Variation in Growth and Facilitates Interpretation of an Early Pliocene Alligator

---

A thesis

presented to

the faculty of the Department of Geosciences

East Tennessee State University

In partial fulfillment

of the requirements for the degree

Master of Science in Geosciences

---

by

R. Davis Gunnin

August 2023

Blaine W. Schubert, Chair

Holly Woodward

Joshua X. Samuels

Chris Widga

Keywords: osteohistology, Lines of Arrested Growth, alligator, growth rate, climate, Pliocene

Femoral Osteohistology in American Alligators (*Alligator mississippiensis*) Reveals High Variation in Growth and Facilitates Interpretation of an Early Pliocene Alligator

by

R. Davis Gunnin

Abstract

Histological analysis of long bone thin sections is commonly used to infer growth rates and ecology of extinct vertebrates, particularly within Archosauria. However, most comparative neontological studies have used small samples of captive individuals, limiting the scope of variation. To fill this gap, 44 femoral thin sections of wild *Alligator mississippiensis* were prepared and analyzed. Comparison of slides revealed that larger individuals from cooler climates tend to show more LAGs compared to southerly *A. mississippiensis* of similar size, however, there is considerable variation. This pronounced variation in wild specimens emphasizes the need to use caution when interpreting paleohistological data with little modern comparative samples. Finally, thin sections of early Pliocene *Alligator* sp. fossils from the Gray Fossil Site (GFS), Washington Co., Tennessee were prepared. The GFS *Alligator* grew more slowly than *A. mississippiensis* examined and may have reached reproductive maturity at smaller sizes.

ACKNOWLEDGEMENTS

Deepest thanks to Dr. Blaine Schubert, Dr. Holly Woodward, Dr. Joshua Samuels, and Dr. Chris Widga: for their time, guidance, and enthusiasm in helping me craft this thesis. Special thanks to Blaine for taking a chance with a local highschool student; Josh for teaching me to think statistically; Holly, for her hospitality in Tulsa and guidance in the field of paleohistology. Season Nye, for her help in collections and encouragement over the years and teaching me to respect all things old. Shawn Haugrud, for introducing me to paleontology. Brian Compton, for taking care of the modern Georgia specimens in this thesis, and all help with the modern collections. Laura Emmert, for her help in processing North Carolina, South Carolina, and Arkansas alligator specimens. Cordray’s Processing and Taxidermy, who graciously donated specimens from South Carolina for this project. Alicia Davis and Liz Scarlett of the North Carolina Wildlife Resource Commission, who facilitated important comparisons with the northernmost alligator populations possible. My parents, Robbie and Sarah, for cultivating my passion for the natural world, especially here in southern Appalachia. My grandparents Tava & Steve for buying so many orchids and exposing me to the biodiversity of north Florida; Ed & Betty, both former schoolteachers who were thrilled to see me pursue a higher education, for their enthusiasm and support over the years. Elliot Fry, for sharing untold evenings in eastern hardwood forests. Matthew Inabinett, for our many illuminating conversations covering the range of vertebrate biology. My fellow students, for the evenings of raucous and enlightening conversation, without which this thesis would be in poorer condition. Sundew, the parrot, for honing my skills in finding errant typos. Finally, my fiancé, Shay Maden, for her partnership and invaluable impact on the way I think about biology.

TABLE OF CONTENTS

LIST OF TABLES

LIST OF FIGURES

CHAPTER 1. INTRODUCTION

Bone histology of fossil archosaurs is commonly used to reconstruct ecology, growth rates and life histories (Padian and Lamm 2013). Annual growth marks in long bones, formed by the complete arrest of growth (called lines of arrested growth; LAGs) are used to reconstruct yearly growth of extinct taxa (Castanet et al. 1993; Padian and Lamm 2013). However, relatively few studies have examined broad scale variation in LAG formation among living, wild archosaurs (Garcia 2011; Padian and Lamm 2013). The lack of comparative data in modern taxa, for which a wealth of associated environmental data is available, has led to poorly justified assumptions regarding LAG formation in extinct taxa (Cullen et al. 2021). This thesis examines variation in femoral LAGs of wild American Alligators (*Alligator mississippiensis*) from several localities across the species' range, including those from the interior of the United States and captive, pen-raised specimens.

Growth and Growth Marks in Limb Bones

Bone is a dynamic living tissue responsible for structural stability, locomotion, and numerous homeostatic functions in vertebrates (Andronowski et al. 2018; Currey 2002; Padian and Lamm 2013). As bone grows materials need to be added, removed, and remodeled (Currey 2002; Sims and Gooi 2008). The first stage of osteogenesis in limb bones begins within the embryo when chondrocytes form a cartilaginous template for the bone (Bruder and Arnold 1989). Endochondral ossification then occurs as the diaphysis of this template is vascularized and impregnated with osteoid, the tissue which is mineralized to form mature bone tissue (Bruder and Arnold 1989; Currey 2002). Osteoid is also formed early at the metaphyses and continues to produce bone tissue in order to lengthen the element (Bruder and Arnold 1989;

Smith and Hall 1990; Currey 2002). To increase cross-sectional area as the bone lengthens, osteoid is produced at the periosteum (Smith and Hall 1990; Currey 2002).

Growth is controlled by the interactions between bone-destroying (osteoclast) and bone-forming (osteoblast) cells (Currey 2002; Sims and Gooi 2008). Osteoclasts are large, multinucleate cells which dissolve both organic and inorganic material (Currey 2002; Sims and Gooi 2008; Padian and Lamm 2013). Osteoblasts work in concert to deposit bone, first as collagen fibrils (osteoid) which are then secondarily mineralized with carbonated hydroxyapatite (Currey 2002; Sims and Gooi 2008; Padian and Lamm, 2013). Some of these cells are entombed in the newly formed bone becoming osteocytes but remain connected to one another by tiny channels called cunaliculi. Bone that grows rapidly, such as in juvenile or endothermic amniotes, tends to be highly mineralized with randomly oriented collagen fibrils and hydroxyapatite mineral plates (Francillon-Vieillot et al. 1990; Currey 2002; Padian and Lamm, 2013). Conversely, more slowly growing bone is laid down as sheets of osteoid, oriented parallel to the surface of the bone similar to the orientation of wood fibers in plywood (Francillon-Vieillot et al. 1990; Currey 2002; Padian and Lamm, 2013). This bone is generally less mineralized but has been shown to have more tensile strength (Currey, 2002).

During periods of lowered metabolic state primary bone growth will slow, resulting in a transition from rapid bone growth to slow bone growth and a concomitant transition in bone tissue type (Francillon-Vieillot et al. 1990; de Margerie 2002). Many, if not most, tetrapods experience this cyclic deposition of osteoid and form distinctive lamellae in their bones which can be seen when viewing a long bone in the transverse plane (de Ricqlès 1976; Francillon-Vieillot et al. 1990; Köhler et al. 2012; Padian and Lamm 2013). The typical method of investigation, osteohistology, uses slices of bone polished to micrometer-scale thickness which are viewed with a standard petrographic (or similar) microscope. Tetrapod stylopodial bones are well suited, as they need to support the animals' mass and withstand compressive, tensile, and rotational forces (Currey 2002). These limitations, as well as unique historical phyletic events, have formed a relatively simple columnar diaphysis with few asymmetries in radial growth. These attributes make long bones such as the femur and humerus particularly useful for assessing skeletochronology and growth rate using periodic growth marks (called circumferential growth marks; CGMs) (de Ricqlès 1976; Francillon-Vieillot et al. 1990; Padian and Lamm 2013). Since CGMs represent the periosteal surface at different intervals over the course of an animal's life, data regarding their dimensions can be used to infer other aspects of bone size and shape (de Ricqlès 1976; Padian and Lamm 2013). Ultimately, rate of change in mass of the entire animal can be inferred from the apposition of bone between preserved CGMs (Padian and Lamm 2013). Remodeling of cortical bone and expansion of the medullary cavity can obscure or completely obliterate evidence of CGMs (Padian and Lamm 2013).

In cases where growth stops entirely CGMs are interpreted as lines of arrested growth (LAGs) and have been shown to be the result of annual states of lowered metabolism which result in complete cessation of bone growth with subsequent resumption (Köhler et al. 2012; Padian and Lamm 2013; Hinrichs 2016; Woodward 2019). The periodicity of LAG formation allows the design of longitudinal studies assessing growth rates of individual bones in an organism, results of which are often assumed to represent somatic growth. The vertebrate fossil record is well suited to osteohistological analyses of LAG formation, which can provide a wealth of data about growth and growth rates for organisms which cannot be directly observed (Padian and Lamm 2013). While LAGs have been documented in many tetrapod taxa, extant and extinct, and have been the subject of numerous paleontological studies (Castanet et al. 1993; Klevezal

1996; Currey 2002; Padian and Lamm 2013), comparatively few neontological studies have examined variation in LAG formation at large geographic scales (Garcia 2011; Köhler et al. 2012; Padian and Lamm 2013). To soundly apply the techniques of osteohistological analysis in the study of fossil taxa, specifically the use of LAGs to infer paleobiology and growth rates of extinct archosaurs, a thorough understanding of bone growth and the abiotic factors that influence it in extant relatives is necessary. To help develop this understanding and build upon the body of neontological osteohistology this thesis examines geographic variation in femoral LAGs in the poikilothermic archosaur *Alligator mississippiensis*.

Alligator Osteohistology

Crocodilians are one of two extant archosaur groups and have been the subject of several neontological osteohistology publications (e.g., Hutton 1986; Tucker 1997; Horner et al. 2001; Lee 2004; Tumarkin-Deratzian et al. 2007; Garcia 2011; Woodward et al. 2011; Woodward et al. 2014; de Andrade et al. 2018; Rainwater 2022). In addition to representing an extant outgroup for investigating osteohistology in non-avian dinosaurs, crocodilians provide more direct information relevant to the study of closely related extinct suchians. Much of the osteohistological baseline work on extant crocodilians has been with the American Alligator, *Alligator mississippiensis* (e.g., Lee 2004; Klein et al. 2009, Garcia 2011; Woodward et al. 2011; Woodward et al. 2014; Rainwater 2021), specimens of which are generally easy to acquire in the United States. Apart from the ubiquity of this taxon, the American Alligator is one of two extant temperate crocodilian species (along with the Chinese Alligator, *A. sinesis*) which presents a unique opportunity to examine the influence of high latitude climatic and environmental conditions on bone growth in archosaurs with poikilothermic metabolisms.

Most osteohistological studies of alligators have focused on one or a handful of, usually, captive or pen raised specimens (Garcia 2011; Lee 2004; Rainwater et al. 2021; Woodward et al. 2014). The largest published study (Woodward et al. 2011) used a group of 30 captive born, pen-raised alligators (*A. mississippiensis*) from Rockefeller Wildlife Refuge (RWR) in coastal Louisiana. Alligator material from RWR has been used in many studies of alligator osteohistology and growth (e.g., Seebacher et al. 2003; Lance 2003; Farlow et al. 2005; Woodward 2011; Ikejiri 2012; Woodward et al. 2014). The histological sections from the RWR femur dataset confirmed in *Alligator mississippiensis* the presence of an external fundamental system (EFS) (Woodward et al. 2011), a type of dense laminar bone growth at the periosteal surface associated with skeletal maturity in amniotes (Andrade et al. 2015; Kolb et al. 2015; Heck and Woodward 2021). The relatively recent confirmation of an EFS in a widely studied living taxon emphasizes the need for large scale neontological studies of osteohistology. Examining variation in large samples of living taxa can reveal previously unrecognized aspects of osteohistology. Such studies are a way to meaningfully understand how factors such as climate and food availability influence bone growth and subsequent histological presentation. Not only can these studies address the biology of extant species, but their findings can also be applied to the fossil record to provide a deeper and more nuanced understanding of the lives of past vertebrates.

Gray Fossil Site Geologic Setting

The Gray Fossil Site is a karst fossiliferous deposit located in north-central Washington County, Tennessee, in the valley-and-ridge of the southern Appalachian highlands. The site was discovered in late May of 2000 by employees of Summers-Taylor, Inc., contracted by the Tennessee Department of Transportation (TDOT) to perform remedial roadwork (Clark et al.

2005). A 20-30 m tall hill at the Fulkerson – TN-75 intersection was responsible for a blind intersection and was being graded flat when workers encountered black, clayey sediments containing fossil vertebrate material (Clark et al. 2005). Subsequent geological and paleontological investigation of the site has interpreted GFS as the remains of several paleosinkholes that filled with water following roof-collapse and coalescence, as evinced by gravity surveys, laminated silts and clays, and abundant fish and aquatic organisms (Wallace and Wang, 2004; Shunk et al. 2006; Whitelaw et al. 2008; Shunk et al. 2009). Inverted topography is accepted as the process that formed the original GFS hill (Clark et al. 2005). As the surrounding Cambro-Ordovician Knox limestone weathered away, insoluble lacustrine sediments protected by a cap of cherty regolith remained as a local topographic high (Clark et al. 2005). Based on mammalian biochronology, the site is considered to be latest Hemphillian or early Blancan in age, which corresponds to ~4.9 – 4.5 Ma (Samuels et al. 2018, Samuels and Schap 2021). Ecometric estimates of climate at GFS based on fossil rodent and lagomorph dentition (Schap et al. 2021) found a Mean Annual Temperature of 16.8ºC, Annual Precipitation of 1342.6 mm, and a Minimum Temperature of the Coldest Month of 2.6ºC, analogous to present-day Atlanta, Georgia in temperature and Tampa, Florida in precipitation. The presence of frost-sensitive taxa such as *Alligator*, a helodermatid, and the tropical vine *Sinomenium* corroborate these estimates (Mead et al. 2011, Liu and Jacques 2010). The site records a remarkably complete ecosystem from an early Pliocene forested environment. Paleobotanical evidence in the form of macro-fossils and pollen suggest a forest dominated by oak (*Quercus*), hickory (*Carya*), and pine (*Pinus*) (Zobaa et al. 2011; Ochoa et al. 2012, 2016; Worobiec et al. 2013). Herbaceous floristic components are similar to those of other forested environments, while the occurrence of lianas (*Vitis*, *Sinomenium*) point towards a humid, closed forest (Liu and Jacques 2010). When floristic components were compared to modern forests, GFS was interpreted to be most similar to subtropical evergreen and montane tropical forests (Reichgelt et al. 2023). Reichgelt et al. (2023) also estimated climatic parameters for GFS and recovered a mean annual temperature (MAT) of 16.4°C and mean annual precipitation (MAP) of 136 cm. The presence of mole salamanders (*Ambystoma*), *Alligator* (the femoral histology of which is addressed in this thesis), numerous aquatic turtles, bald cypress (*Taxodium*), and tupelo (*Nyssa*) all suggest that the environment was persistently wet (Boardman and Schubert 2011; Worobiec et al. 2013). The GFS *Alligator*, currently identified as *Alligator* sp., is the subject of this thesis and the motivation for compiling a comparative sample of *Alligator mississippiensis* (Blaine Schubert pers. comm.).

Thesis Goals

While osteohistological studies involving captive and pen raised alligators provide valuable control over some environmental factors (such as pathologies and diet), life histories of the specimens do not accurately reflect the conditions experienced by wild animals. Additionally, geographically limited data do not capture the extent of geographic and environmental influences on bone growth in *Alligator mississippiensis*. To explore variation in bone growth within and among populations, this thesis examines femoral histology from a large sample (n = 44) of wild *A. mississippiensis* across their historic geographic range (Chapter 3). These data can provide a foundation for better understanding femoral growth and development in *Alligator* with respect to climatic and environmental variation. In addition, these data can be applied to better understand the paleobiology of fossil archosaurs, such as the early Pliocene Gray Fossil Site *Alligator* examined here in Chapter 3. The following questions provide the foundation and scope for this overall thesis project:

1. How much and what kind of variation in growth-arrest lines (LAGs) is present in extant *A. mississippiensis* across its natural range?

2. How quickly did the GFS *Alligator* grow compared to living *A. mississippiensis*?

3. If the GFS *Alligator* is skeletally mature, is the small size due to local climate or habitat suitability, as in some extant crocodilian populations?

CHAPTER 2. MATERIALS AND METHODS

Modern *Alligator* Specimens

Femora of wild *Alligator mississippiensis* were sampled with specimens procured from the states of Arkansas, Georgia, South Carolina, and North Carolina. Prior to this study East Tennessee State University (ETSU) acquired a large collection (Table 1) of *Alligator* skeletal material from southern Georgia and a limited number from other states, but to address variation in LAGs, more *Alligator mississippiensis* specimens were added to the sample in order to reflect the modern geographic distribution of the species. Wild *Alligator* femora representing the species' continental populations were acquired as a donation from the Arkansas Game and Fish Commission (Table 2). Specimens from South Carolina (Table 3) were from hunters in the low country and were donated by a meat processor. North Carolina specimens (Table 4) were donated by the North Carolina Wildlife Resource Commission (NCWRC) which had been collecting femora from *Alligator* for several years prior to the conception of this study to obtain genetic and skeletochronological data to characterize the states' alligator demographics.

Table 1 Specimens from East Tennessee State University processed into thin sections

Femur ETMNH-Z	**Locality**	**Femur length (mm)**	**Min. Circ. (mm)**
265	AR	257	87
18457	GA	205	68
18464	GA	152	49
18459	GA	224	75
18460	GA	189	60
18461	GA	216	71
3334	GA	158	42

3116	GA	194	63
18458	GA	137	42
3150	GA	133	40
3024	GA	179	57
18432	GA	95	27
5025	GA	94	28
487	GA	144	44
18453	GA	127	38
18433	GA	115	33
18430	GA	154	50
03123	GA	105	32
18452	GA	151	48
18466	GA	171	55
18465	GA	223	73
18468	GA	186	60

Table 2 Specimens from Arkansas processed into thin sections

Femur ETMNH-Z	**CITES tag**	**Femur Length (mm)**	**Min. Circ. (mm)**
20000	NA (road kill)	223	79
20001	AR21-000001	143	44
20003	AR22-000056	128	41
20004	AR21-000002	179	55
20006	AR22-000057	136	45

Table 3 Specimens from Cordray’s Processing and Taxidermy in South Carolina included in this study

ETMNH-Z	CITES tag	Femur Length (mm)	Min. Circ. (mm)
20024	10059	127	41
20025	10497	194	61
20026	10173	245	96

Table 4 Specimens donated by the North Carolina Wildlife Resource Commission. Specimens bolded and underlined are those included in the analysis

ETMNH-Z	NC County	Total Length (cm)	Snout-Vent Length (cm)	Sex	Femur Length (mm)	Min. Circ. (mm)
20020	Brunswick	299.72	142.24	Male	202	79
20021	Duplin	314.96	173.99	Male	224	77
20007	Tyrrell	127	-	Unknown	94	31
20022	Brunswick	248.92	121.92	Male	168	55
20017	Tyrrell	238.76	116.84	Female	165	52
20008	Onslow	156.21	63.5	Male	107	35
20009	New Hanover	203.2	99.6	Female	141	44
20010	Onslow	103.82	51.12	Male	66	21
20016	Brunswick	232.41	125.73	Female	176	60
20023	Columbus	292.1	154.94	Male	199	68
20011	Brunswick	170.2	82.6	Male	116	37
20012	Brunswick	241.94	125.73	Male	172	58
20013	Hyde	161.29	78.11	Male	109	36
20015	Brunswick	210.8	106.7	Female	135	43
20018	Brunswick	277.5	146.4	Male	193	63
20014	Pender	288.3	149.9	Male	196	68

Captive, pen-raised alligators culled from Rockefeller Wildlife Refuge were included in this study as well (Table 5). These specimens were previously prepared according to standard osteohistological techniques at the Museum of the Rockies (MOR).

Table 5 Specimens from Rockefeller Wildlife Refuge included in this study. All specimens are female

Femur #	**Femur Length (mm)**
RWR15	192
RWR20	184
RWR2	181
RWR3	188.5
RWR1	N/A
RWR10	187
RWR30	187
RWR32	192
RWR33	188
RWR36	196

Georgia ETMNH-Z (East Tennessee State University Museum of Natural History, zoology collection) specimens were polished and some preslide wafers were cut (both described below) but embedding, most wafering, and slide mounting was performed at the Woodward Paleohistology Lab at Oklahoma State University-Center for Health Sciences in Tulsa, Oklahoma. Embedding was performed using methods as outlined in Schweitzer et al. 2007 and Woodward et al. 2014.

Although Georgia specimens at ETSU were already cleaned as isolated skeletal elements housed in the ETMNH-Z collection, many specimens from Arkansas, North and South Carolina remained as either intact limbs or isolated bones with varying amounts of soft tissues. Limbs from these samples underwent manual de-fleshing, followed by further processing in a dermestid beetle colony, the larvae removing much of the remaining soft tissues. In some cases, dried epiphyseal cartilage was avoided by the beetles, so specimens were occasionally rehydrated to facilitate consumption by dermestid larvae. Some South Carolina specimens were water macerated over the course of summer 2022.

After manual de-fleshing, beetle processing and/or maceration and final air drying, standardized femoral measurements of length and minimum circumference at the mid diaphysis (minimum mid-diaphyseal circumference; MMDC) were taken following methods used in Farlow et al. 2005. The minimum circumference of the mid-diaphysis was measured using a tailors' tape (12mm wide). This minimum circumference along with standard anatomical orientations were drawn onto the section of bone to be removed using a #2 pencil. After labelling with pencil, the 2-3 cm section at the mid-diaphysis was cut out using a water-cooled tile saw equipped with a diamond blade.

These initial sections were chemically processed in preparation for embedding in resin. Sections were soaked in a 1% solution of Tergazyme® detergent for at least 5 days at temperatures from 20C – 40C until medullary tissue was soft enough to be easily removed and the bone tissue showed signs of lipid solubilization (e.g., increased translucence). Sections were allowed to soak in Tergazyme® for at least one day after removing medullary tissue. Sections were then rinsed under tap water and submerged in a 10% buffered solution of formalin for 3 days. Once fixed in formalin, sections were rinsed and dehydrated in ethanol solutions of increasing concentrations: ~70% for 3 days, ~80% for 4 days, and finally 95% for one week. After ethanol dehydration sections were air-dried under a fume hood for 1-2 days. Prior to embedding sections were also desiccated with anhydrous calcium sulfate (Drierite™) for several hours. When fully dehydrated and ready for embedding, faded pencil labels were retouched and a red dot was marked on the distal face of the cut section using a wax or china pencil.

Samples were embedded with Silmar® 41 clear polyester resin catalyzed with methyl ethyl ketone peroxide (MEKP). In some of the first embedded samples, latex mold release was used to facilitate removal, but no difficulty was encountered when removing blocks that lacked mold release, so this step was skipped in subsequent embeddings. Bone sections were glued to a >1 cm thick precured resin base with thin cyanoacrylate glue. Specimens were oriented with the periosteal surface towards the base, as opposed to the cut surface. In later embeddings the precured base was made exclusively using excess resin trimmed from completed blocks; trimmed pieces were also used as bulk to reduce the amount of resin needed to embed. A paper triangle indicating specimen identification was also adhered with thin cyanoacrylate near each bone section on the precured base. This triangular label pointed distally, providing information that was redundant to the red wax/china pencil marking. After the specimen and label were affixed to the precured base, catalyzed Silmar® resin was slowly poured into the embedding container until sections were submerged by 1-2cm. Embedding containers were then placed in a Fisher Isotemp® vacuum oven under -27” Hg for ~15 minutes, or until bubbling slowed/ceased. One batch of embedded sections was pulled from vacuum early (before bubbling had ceased) due to high air temperature accelerating the resin curing process. Vacuum was slowly released to allow even resin impregnation and embedded sections were then placed in a refrigerator (3-5 °C) for ~24 hours to slow the curing process and allow any remaining bubbles to rise to the surface. After refrigeration resin blocks were placed under a fume hood to finish air curing at 23 °C – 32 °C.

Fully cured resin blocks containing embedded sections were trimmed of excess resin using a tile saw with a diamond blade (trimmed excess was saved for future embedding; see above). Trimmed blocks were then labelled with a Sharpie® permanent marker indicating anatomical orientation and identification. Lines of three different marker colors were drawn diagonally along the resin block to aid in identifying cut-order if multiple slides were made from the same block. Since preslide wafering was to be performed with a Model 65C Ingram Thin Section Saw/Grinder, which uses a vacuum chuck to mount petrographic slides, glass or acrylic slides were glued with cyanoacrylate to the distal or proximal end of the resin block. A ~2mm thick preslide wafer was removed at the minimum mid-diaphyseal circumference of the embedded bone with the Ingram thin section saw. These preslide wafers were then adhered with cyanoacrylate to acrylic slides that were pre-polished with 600 grit carbide paper to facilitate adhesion. After allowing the cyanoacrylate glue to cure for 48 hours, slides were polished using successively finer (600, 800, and 1200 grit) carbide polishing papers on a Buehler Ecomet™ III Polisher-Grinder until LAGs and microscopic features of the bone tissue were visible (typically 80 – 150 µm thick). Five-micron aluminum oxide polishing powder was used to remove marks from the final 1200 grit polishing. Finally, Permaslip® liquid coverslipping medium was applied to the thin sections to protect exposed bone from damage and prevent slide cracking. Some embedded specimens trapped air during mounting and retained one or more bubbles between wafer and acrylic slide after the cyanoacrylate was cured. In such cases, normal polishing could result in the thin section tearing, perforating, or being completely polished away at the site of the trapped bubble. This was an increased risk when the trapped bubble was large enough to allow the thin section above the bubble to “bow out” of the slide plane. Final polishing of these specimens, would allow aluminum oxide to enter the bubble space and block transmitted light from the microscope stage, thus preventing interpretation of local bone tissue features. To avoid this, the polishing procedure was modified for slides with trapped bubbles that were large enough to cause bowing out. The 600 and 800 grit stages were abbreviated, and polishing was mostly performed with 1200 grit. If continued polishing with 1200 grit risked slide perforation, the polishing was considered complete. Despite the slightly ‘frosted’ appearance of the thin section surface when the final aluminum oxide step was omitted, it was found that Permslip® applied normally as with other slides filled these micro-abrasions and resulted in slide clarity similar to that of aluminum oxide polished slides.

To measure LAGs and perform analyses, composite digital photomicrographs were taken using a Nikon Optiphot-2 polarizing microscope mounted with an Accu-Scope® Excelis™ HD microscope camera. Photomicrographs were stitched together from images taken at 40X magnification, using the live image stitching function in the Excelis™ camera software CaptaVision+™. For each specimen two composite photo series were compiled: one in plane polarized light and one in cross polarized light with a full wave plate filter. Plane polarized light typically displays circular growth marks (CGMs) more clearly than circularly polarized light, which reveals birefringent mineralized microstructures within the bone tissue but can often obscure CGMs.

Gray Fossil Site *Alligator* Specimens

To investigate bone histology of the Gray Fossil Site *Alligator*, three femora were analyzed **(**Table 6**)**. These limb elements represent three individuals from across the deposit at varying elevations within the fossiliferous sediments. Limb elements were initially consolidated by Gray Fossil Site preparators using polyvinyl butyral B-98 with 91% isopropyl solvent while broken fossil bone was adhered together using polyvinyl butyral B-76 in acetone solvent. Gray Fossil Site *Alligator* limb elements were processed into histological thin sections in the Woodward Paleohistology Lab at Oklahoma State University-Center for Health Sciences, where embedding, sectioning, polishing, and slide photography took place. Element length and minimum mid-diaphyseal circumference was measured (Table 6) as described above, while anatomical orientations and MMDC were labelled on the bone using a #2 pencil. Unlike the modern bone, the first two cuts into each fossil femur was also indicated with #2 pencil. Sectioning of the whole fossil femora was performed using a Buehler Isomet™ 1000 saw equipped with a 6″ diamond blade. This saw also performed wafering of resin blocks with the embedded fossil bone section. Embedding, wafering, and polishing was completed largely as described above, apart from differences in equipment used. A Buehler Ecomet™ 4 was used to polish fossil slides, starting with 320 grit instead of 600. Aluminum oxide polishing was twofold, with a final one micron polishing step in addition to 5 micron polishing. No coverslip or coverslipping medium was used on the slides. Slides were photographed using a Nikon DS-Ri-2 camera mounted to a Nikon Ni-U Eclipse polarizing microscope. Stitching of full slide photomicrographs was completed automatically by Nikon NIS Elements: Documentation.,

Table 6 Gray Fossil Site *Alligator* femora included in this study

Specimen	**Femur Length (mm)**	**Femur Min Circ (mm)**	**Section Total Area (mm2)**	**Cortical Perimeter (mm)**	**Medullary Cavity Area (mm2)**	**Medullary Cavity Perimeter (mm)**	**Bone Area (mm2)**	**# of LAGs**
ETMNH 82	101	31	111.4	38.58	8.8	11.71	102.6	13
ETMNH 7729	159	52	224.85	53.87	17.8	16.01	207.05	25
ETMNH 18124	138	44	174.02	47.55	8.28	10.95	165.74	24

Data Collection

CGMs that could be interpreted as LAGs were identified and counted for each specimen. The identification of LAGs followed definitions as outlined by Francillon-Vieillot et al. (1990) and Castanet et al. (1993). In cases where LAGs split or merged with another, the two were counted as one and the outermost LAG was used when measuring radial growth (Cullen et al. 2021). In addition to LAG counts, the total area of the femoral cross section was calculated by tracing the periosteal surface using the polygon tool in ImageJ Version 1.53t. The medullary cavity area was calculated using the same method, and from the total thin section area the medullary cavity area was subtracted to result in the bone area of the thin section. The geometric centroid of the periosteal (total thin section) polygon was calculated, as well as that of the medullary cavity polygon. To record growth of each *Alligator* femur, the radial distance to each LAG from the total area centroid was measured to the nearest hundredth of a millimeter using ImageJ Version 1.53t, culminating in the distance from the centroid to the periosteal surface (the complete radius of the thin section). To ensure that measurements were made along the same axis for each specimen, all radial measurements were taken along a line extending from the centroid to the maximum curvature of a distinct inflation of the periosteal surface (Figure 1).

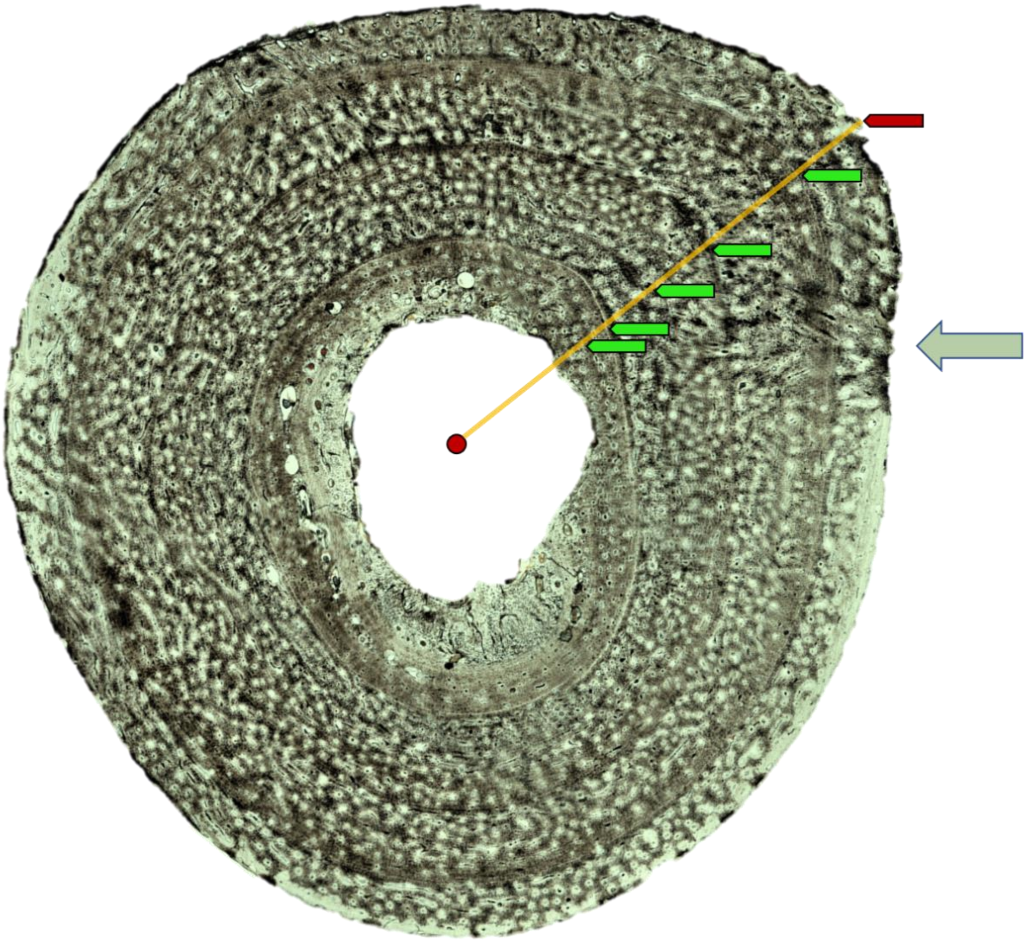

Fig. 1 Location of measurements taken from femoral thin sections. Gray arrow indicates attachment of *M. femorotibialis externus*, red dot is the periosteal centroid, green arrows mark LAGs, red arrow is the periosteal surface.

This inflation is readily identifiable in every mid-diaphyseal thin section and occurs just laterally to a region of radially oriented vascular canals that correspond to the ventral-most attachment of the *M. femorotibialis externus* (Petermann and Sander 2013). From these values, not only can cumulative radial growth be plotted as a time series, but inter-LAG distance is easily calculated.

Analysis of Data

Data were analyzed using Microsoft Excel Version 2304 and SPSS Version 29.0. For each slide, bone area (BA), medullary area (MA), and total thin section area (TA) were plotted against one another and against femur length. A least squares regression was performed to describe relationships between the thin section metrics, as well as thin section metrics and femur length. The square root of areal measurements was regressed against femur length to produce a linear relationship.

To infer femoral growth rates and compare them among specimens, femoral length (a good proxy for body mass; Farlow et al. 2005) was plotted against the number of LAGs identified in each specimens' thin section. This simple method provides direct comparison of similarly sized femora and allows the inference of growth rates; specimens of similar size but with a different number of LAGs are assumed to be growing at different rates. The average inter-LAG distance was also calculated for each specimen and plotted against femur length to compare inferred growth rates. Comparison is made between alligators of similar size. Individuals with a more rapid growth rate will deposit more bone per growing season, resulting in a larger inter-LAG distance. Note that these two methods are closely related, as specimens with more LAGs should have a shorter average inter-LAG distance. In both cases the x-axis was chosen to represent femur length, primarily for ease of interpretation. Cumulative radial growth of the femur along one axis (from the centroid to the periosteal surface, as described above) was plotted as a time series for each measured specimen as well, with each time interval assumed to represent one year. Descriptive statistics, Levene's test for variance homogeneity, and independent samples T-tests were performed for the two largest groups: North Carolina and Georgia alligators. Statistical analysis was performed on inter-LAG measurements scaled to the largest thin section in the study. Scaling used the square root of the area of the total thin section of (ETMNH-Z number).

CHAPTER 3. RESULTS

Thin Section Areas

In all cases total thin section area and bone area have similar relationships with the other variables. Dependance of bone area values on total thin section area – bone area being the total thin section area minus the medullary cavity area – results in this similarity.

Unsurprisingly for a weight bearing bone, square roots of total thin section area and bone area (Figures 2 and 3, respectively) are closely linearly correlated with femur length, itself a close correlate with body mass.

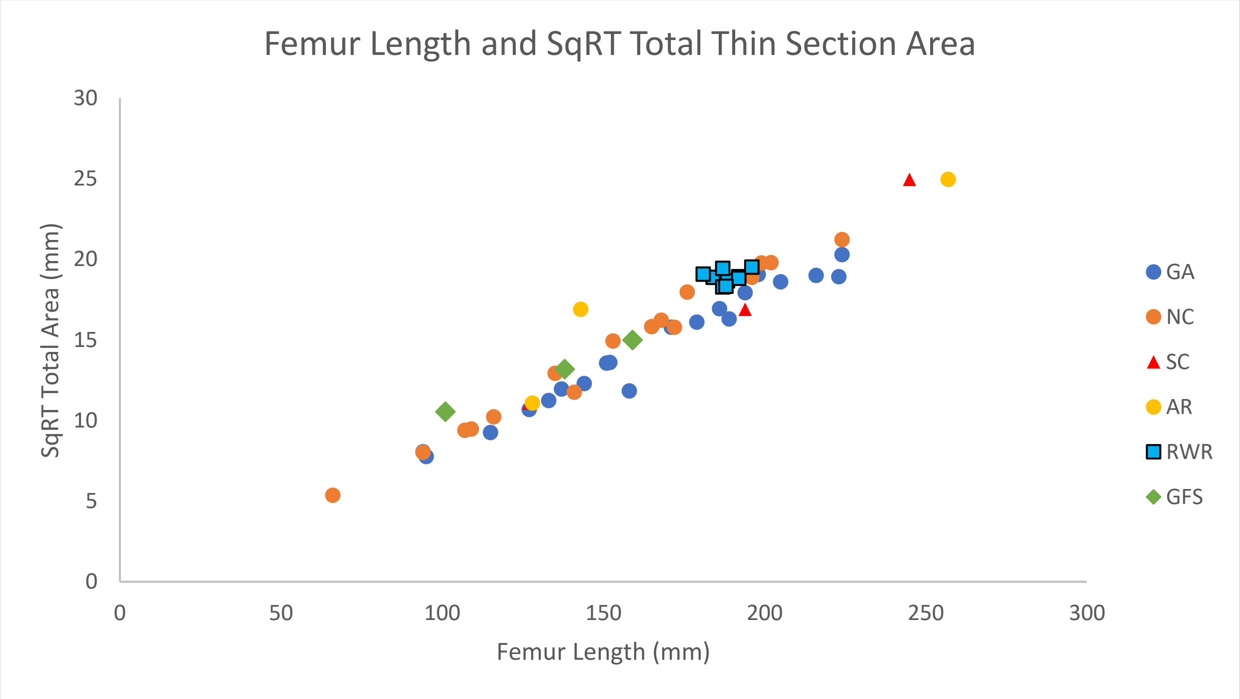

Fig. 2 Bivariate plot of femur length and square root of total thin section area.

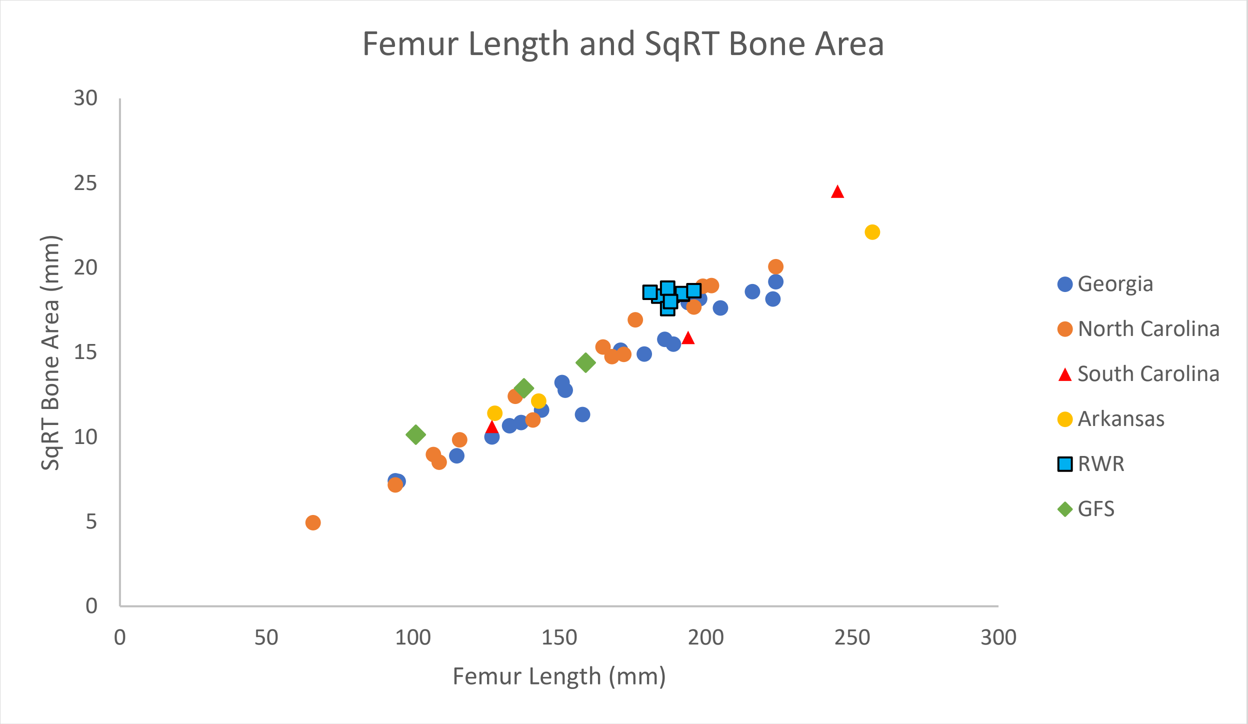

Fig. 3 Bivariate plot of femur length and the square root of bone area.

Unlike the relationships between total thin section or bone area and femur length, which show close correlation, that between medullary area and femur length is weaker (Figure 4). Note that the pen-raised female alligators from Rockefeller Wildlife Refuge (RWR), all about the same size and age at death, lie along a different slope than the wild specimens included in this thesis. Variation in the RWR sample is mostly in area of the medullary cavity, rather than length of the femur.

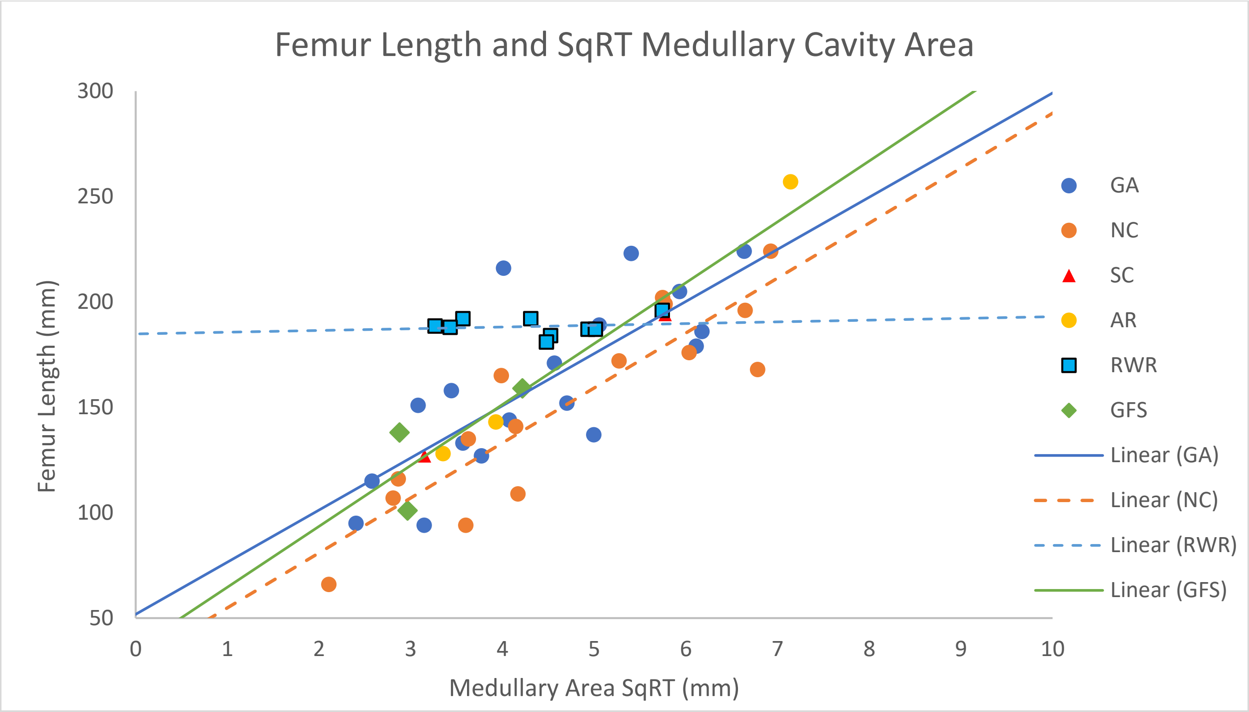

Fig. 4 Bivariate plot of femur length and the square root of medullary area. Linear equations are fit to alligators from each U.S. state and GFS.

Similarly, total thin section area and medullary area show a weak linear relationship (Figure 5).

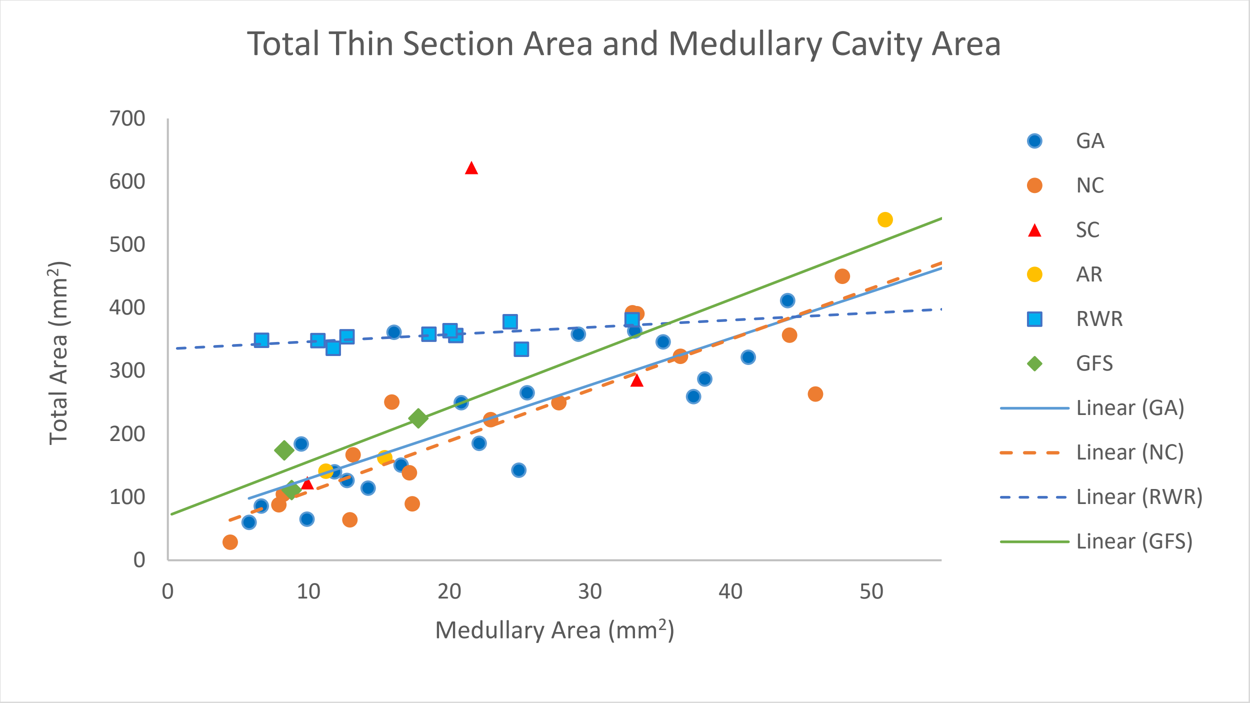

Fig. 5 Bivariate plot of total thin section area and medullary cavity area. Linear equations are fit to alligators from each U.S. state and GFS.

The relationship between bone area and medullary area (Figure 6) is comparable to that between total thin section area and medullary area due to the non-independence of the two values. The pen-raised Rockefeller Wildlife Refuge specimens are again seen to follow a different slope than the wild specimens, showing variation in medullary area but little deviation in bone area.

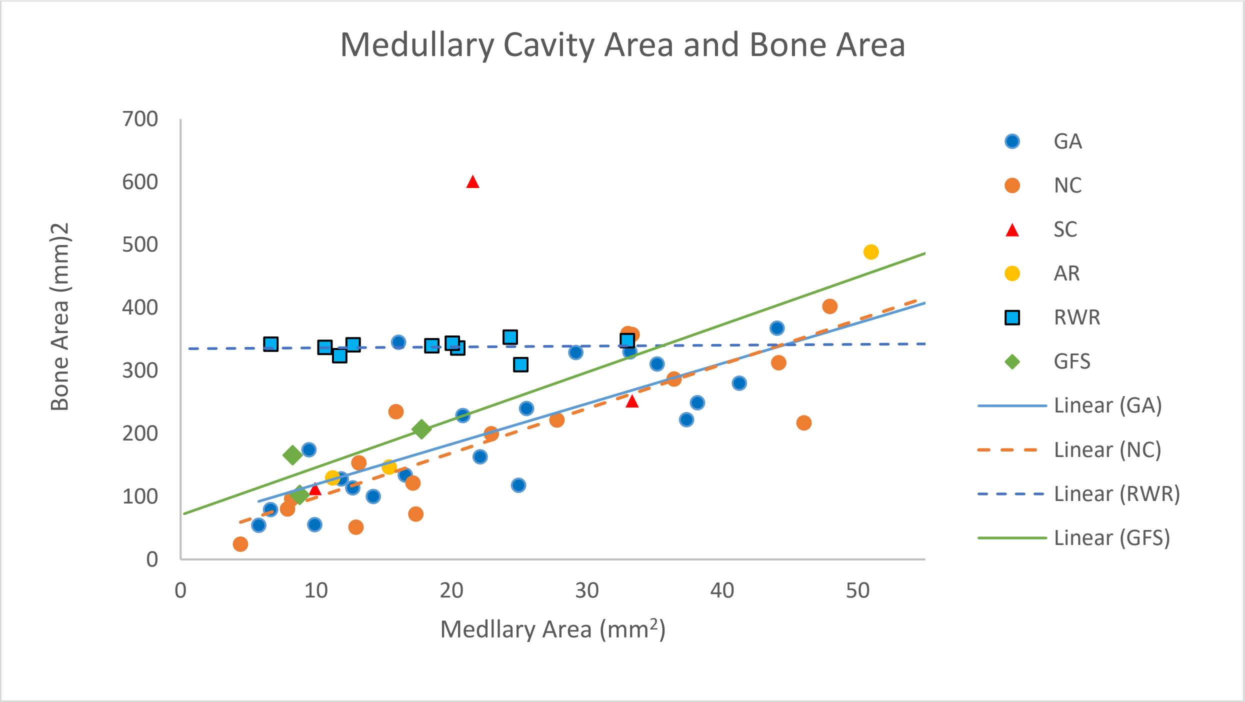

Fig. 6 Medullary cavity and bone area plotted against one another with linear equations fit to each alligators from each state

Total thin section area and bone area, values differing only by difference of the comparatively smaller value of the medullary area, show a close linear relationship (Figure 7). The remarkably close correlation results from the bone area and thin section area being non-independent values.

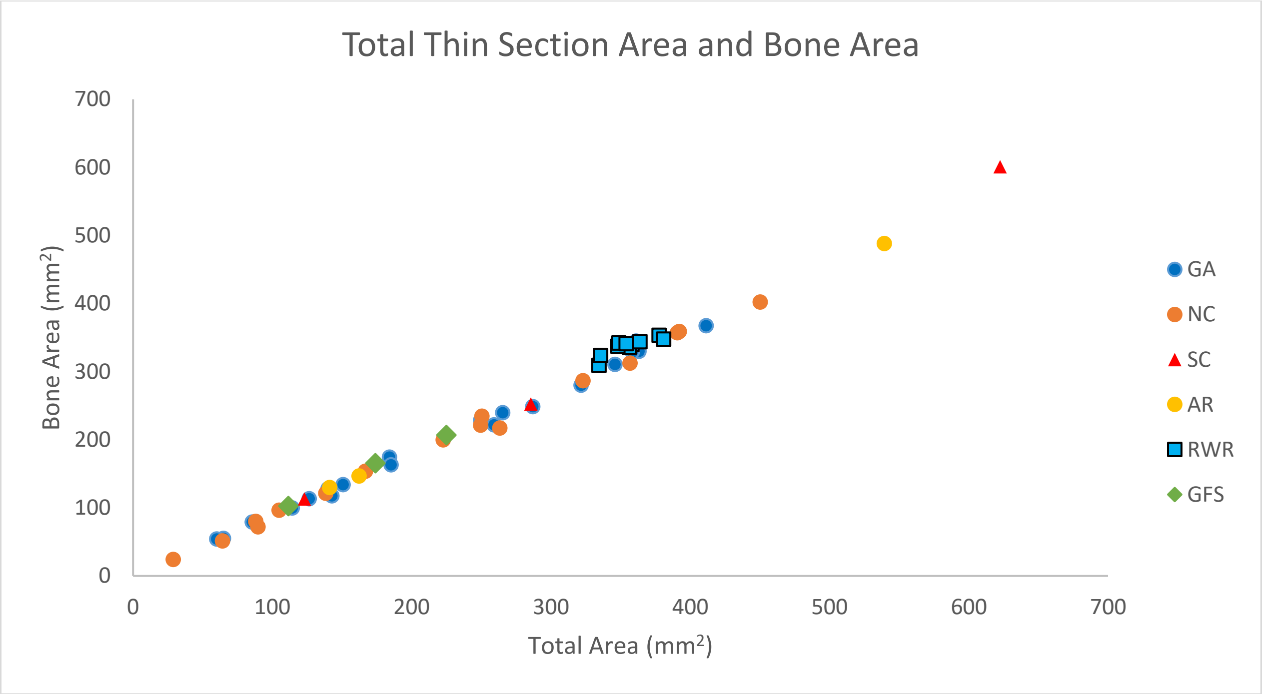

Fig. 7 Bivariate plot of total thin section area and bone area.

<u>LAG Counts and Femur Length</u>

As shown below in Figure 8, the slope of the Georgia femur sample is shallower than that of the North Carolina sample (GA = 0.027; NC = 0.084), with an intercept between the two at ~115mm of femur length. Below this size, North Carolina femora are predicted to have fewer LAGs than those from Georgia. Alligator femora from Arkansas and South Carolina also tend to have higher LAG counts than those from Georgia. All of the RWR femora are of similar size and age, so variation in LAG counts spreads the data along the y-axis.

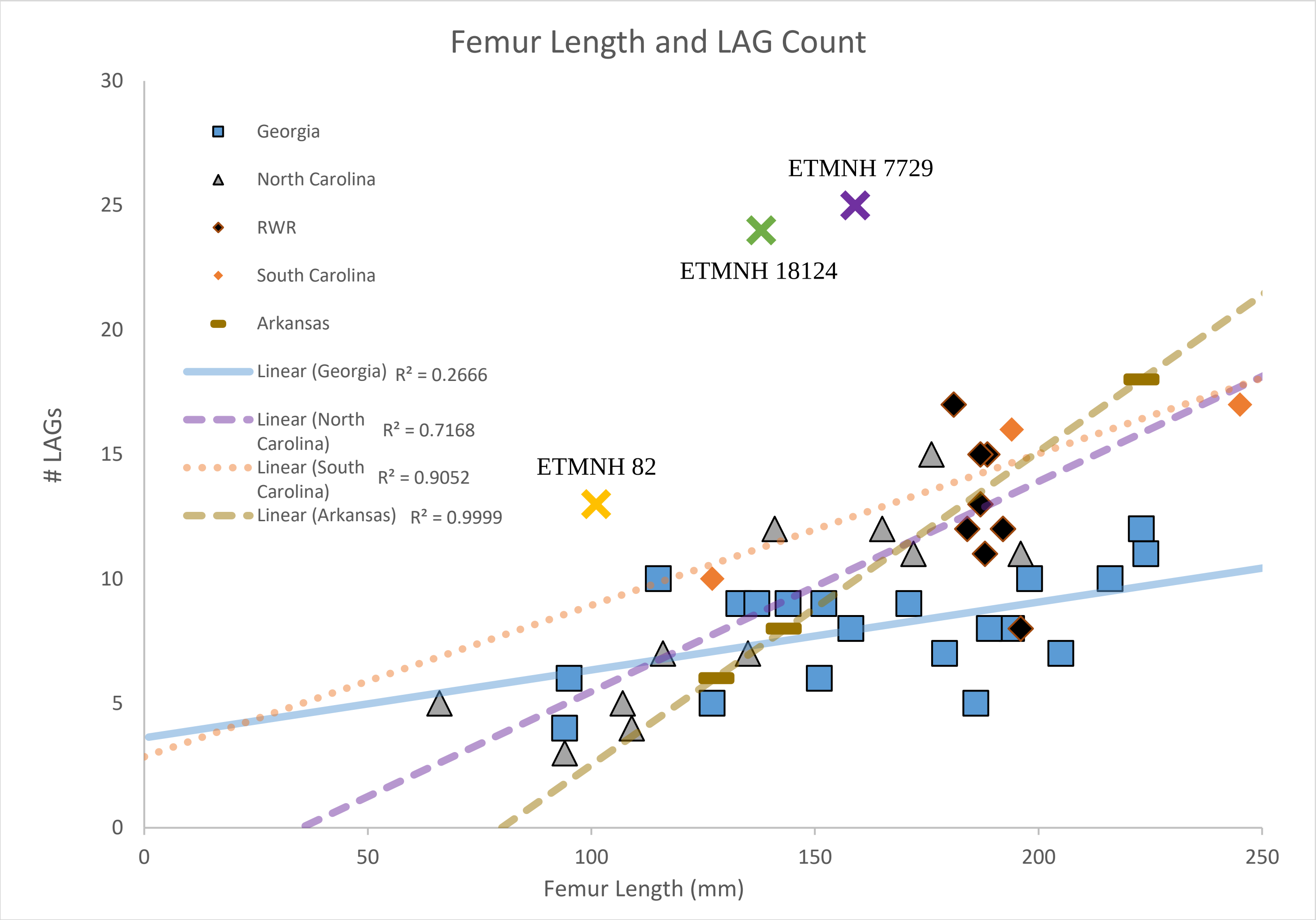

Fig. 8 Bivariate plot of femur length compared to LAG counts in wild and captive *Alligator mississippiensis*. Gray Fossil Site *Alligator* femora are indicated by their catalog numbers.

Inter-LAG Distance

Inter-LAG spacing is more variable against femur length compared to LAG counts, but the eight Georgia femora measured have greater LAG spacing than eight of 13 measured North Carolina specimens. Compared to femora from wild *A. mississippiensis*, GFS *Alligator* femora have the narrowest inter-LAG distance. RWR femora have similarly narrow LAG spacing, but as noted above this is likely due to the advanced ontogenetic stage and formation of an EFS skewing the mean inter-LAG distance to the left.

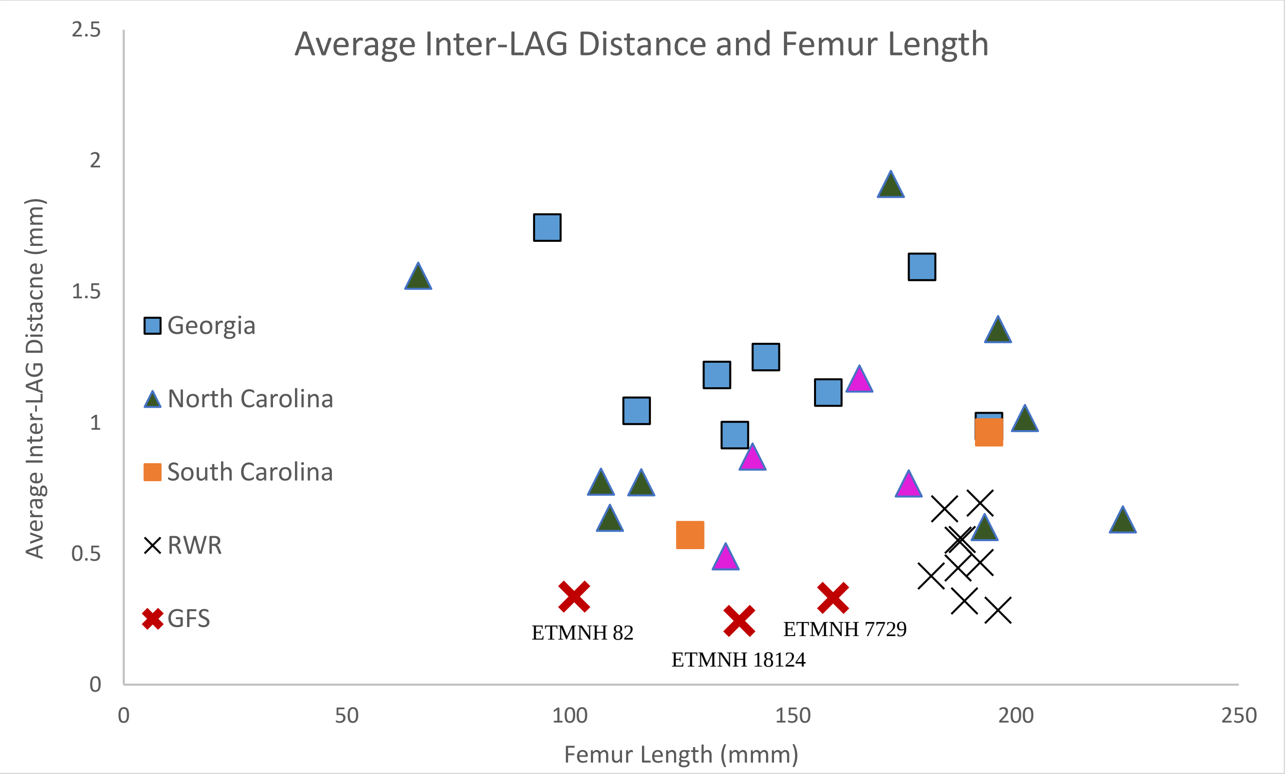

Fig. 9 Bivariate plot of average yearly apposition (inter-LAG distance) and femur length. Magenta triangles are female North Carolina specimens. All RWR specimens are female. No other specimens had sex data associated.

Levene's test for equality of variance indicated that the two samples (North Carolina and Georgia) had equal variance (p = 0.135). The t-statistic significance level was p = 0.740 and the confidence interval crossed zero, strongly suggesting that the mean inter-LAG distances for specimens from North Carolina and Georgia was not significantly different. Results of these statistical tests are reported below in Table 7.

Table 7 Results of an independent samples t-test between Georgia and North Carolina scaled inter-LAG measurements

Levene's Test		**Independent Samples Test**					**95% Confidence Interval of the Difference**	
F	Sig.	t	df	Two-sided p	Mean Difference	Std. Error Difference	Lower	Upper
2.442	0.135	0.336	20	0.740	0.09523	0.28340	-0.49594	0.68640

CHAPTER 4. DISCUSSION

The femoral thin sections analyzed in this study reveal considerable variation between modern American alligators from different regions, however, some general trends in LAG formation can be identified. Scaled and unscaled inter-LAG distance appears to be a poor proxy for inferring growth rates between individuals. Calculating a coefficient of variation shows that average inter-LAG distances are subject to considerable variation between specimens (CoV GA = 0.53; CoV NC = 0.55). The reason that inter-LAG distances show such variation may be due to the non-linear nature of bone growth, such that inter-LAG distances in very young and very old individuals can be similar due to slow growth during both ontogenetic stages. In contrast, comparison of LAG counts between similarly sized individuals provides a better inference of bone growth rate. Since this method does not rely on LAG metrics, merely the number of LAGs recorded in each femur, asymmetric ontogenetic growth as described above does not directly introduce variation in growth rate inference. Comparing LAG counts between similarly sized femora from different climatic regimes (i.e. North Carolina, Georgia) shows that more southerly alligators record a more rapid growth rate in osteohistological thin section, in agreement with non-histological data demonstrating differing growth rates between populations (Lance 2003). This inferred difference in growth rate is most apparent among more mature individuals, corroborating past work which suggests that osteohistological growth rate is best captured in thin sections from the stylopodial bones of mature individuals (Cullen, 2021). Still, variation in LAG counts between individuals is subject to non-negligible variation, possibly due to localized environmental conditions such as food availability which may overcome the effects of large-scale climatic trends. Care should be taken to consider such sources of variation when inferring growth rates of stylopodial bones using LAG counts.

Comparison of the three fossil Gray Fossil Site (GFS) *Alligator* femora with extant specimens included in this studied revealed a considerably slower inferred growth rate for the fossil form. The GFS slides had the most LAGs of any femur examined, and when compared to similarly sized *A. mississippiensis* the GFS femora exhibited highly elevated LAG counts. Mean inter-LAG distances of the GFS *Alligator* were also narrowest compared to all wild *A. mississippiensis*, though some of the captive *A. mississippiensis* had comparably narrow (or narrower) inter-LAG distances, possibly due to their advanced ontogenetic stage skewing the data left (towards less yearly apposition).

The slow growth rate of the GFS alligator could be due to external or internal factors. Externally, local climate and food availability can constrain growth. The markedly similar mean annual temperature (MAT) of coastal North Carolina (where several comparative femora are from) to the estimated MAT for GFS seems to suggest that climate is not responsible for the slower growth rate in the GFS fossil alligator. However, as semi-aquatic animals, alligators are sensitive to water temperature, which can also affect growth rate (Nickum et al. 2018). Unlike coastal North Carolina where water temperature can be stabilized by oceanic climatic influence, an inland karst feature like the Gray Fossil Site may have had significant influence from cool groundwater, which could limit the maximum temperature of the sinkhole lake water. Cool groundwater may have acted to retard growth of the GFS fossil alligator. The presence of ample prey species available to the GFS *Alligator* (when assuming *A. mississippiensis* dietary preferences) would also suggest that limited food resources are not responsible for a slower growth rate. However, no data is available for population density estimates of prey species, so despite the presence of suitable prey taxa, low densities of these taxa could result in slow growth.

Internally, sexual dimorphism may explain the slow growth rate of the GSF fossil alligator. However, dimorphism in growth rate of the GFS alligator would need to be far more pronounced than in the living *A. mississippiensis*, and all three fossil femora examined would need to be the same sex. Since this study did not test for differences between male and female specimens a pronounced sexual dimorphism in the fossil taxon cannot be ruled out. Alternatively, I interpret the slow growth rate of the GFS *Alligator* as being an endogenous, phyletic trait. The slower growth rate inferred from femora of the GFS *Alligator* contributed to smaller adult body sizes of this taxon when compared to *A. mississippiensis*. A transition from small to large adult body size occurred within *Alligator* in the late Cenozoic (Hastings et al. 2023), and the more rapid growth rate of *A. mississippiensis* compared to the GFS fossil taxon may indicate a heterochrony that helped achieve an increase in adult body size within the *A. mississippiensis* lineage.

Thin Section Areas

This thesis examines the relationships between bone area, medullary cavity area, total thin section area, and femoral length for a large sample of wild *Alligator mississippiensis*. These relationships probably reflect the load-bearing properties of femora (Currey 2002; Lieberman et al. 2004). However, some relationships (especially those regarding the medullary cavity) could be the result of sexual dimorphism. This study did not test the effects of sexual dimorphism in femoral thin section metrics. Medullary cavity area was poorly correlated with femur length and the other area measurements, but total thin section area and bone area were closely correlated with each other and with femur length. Due to the medullary area being so small compared to total or bone area, and that bone area is calculated by subtracting medullary area from the total area, bone area and total area were closely correlated ($R^2 = 0.99$) linearly. Bone area and total area were both closely correlated with femur length, which is likely due to the mechanical requirements for load bearing in this bone. The pen-raised alligators from Rockefeller Wildlife Refuge (RWR) were all the same age, sex, similar sizes, and plotted as outliers compared to the wild sample. The RWR alligators had more variable medullary cavity area despite being the same sex, age, and similar to one another in size. It is unclear why this variation is present, but it could be due to variation in thin section sampling location along the femur.

Modern *Alligator*

Long bone histology is frequently used to reconstruct growth rates in fossil archosaur taxa (Padian and Lamm 2013), but neontological studies of extant relatives exploring histovariability and/or testing assumptions made by past workers are comparatively lacking (Garcia 2011). Thus, this thesis attempted to assess histological growth rates in femora of *Alligator mississippiensis* using comparison of LAG counts and length measurements of the femur (a close correlate with mass; Farlow 2005). It is well known that crocodilian growth rate varies according to several environmental factors such as temperature and quality of habitat (Murphy 1977; Jacobsen and Kushlan 1989; Lance 2003). Indeed, it seems that controls on growth rate vary from population to population (Jacobsen and Kushlan 1989; Lance 2003). Broadly, food availability and temperature are thought to play an important role in controlling how quickly crocodilians can grow (Jacobsen and Kushlan 1989; Shine 2001; Lance 2003).

Due to the non-linear nature of vertebrate bone growth (Cullen et al. 2021) direct comparison of bod size measurements of *Alligator* at different ontogenetic stages risks erroneous conclusions due to differential growth rates. Commonly used models describe growth as slow in both early and late ontogeny with rapid growth between (Padian and Lamm 2013; Cooper et al. 2018). When comparing measurements of growth rates between individuals it is important to compare those that are at the same (or similar) ontogenetic stage to reduce bias introduced by differences in relative growth rate caused by ontogeny. Femur length was plotted along the x-axis and all LAG metrics on the y-axis; this allows direct comparison of similarly sized individuals. A regression line could then be fitted to specimens to help visualize differences in inferred growth rate. This method does not directly model or attempt to quantify rate of growth, but instead compares relative growth rate based on the assumption that a more slowly growing individual will have more LAGs and/or less distance between them than a more rapidly growing individual of the same size.

Although broad relationships between femur length and LAG counts are present in these data, there is considerable overlap in the inferred growth rates of the alligators included in this study. In graphs comparing femoral length and the number of LAGs, Georgia alligators tended to have fewer LAGs as femora passed 115mm in size, whereas below 115mm North Carolina alligators had more LAGs. This interpretation is based on the intercept of the regression lines for each group (NC and GA). However, there were only two North Carolina alligators with femora <115mm, so any conclusions drawn from this apparent inversion should be considered tentative due to the small sample size. At larger sizes there is a clear distinction in LAG counts between femora from different localities, further supporting the suggestion that individuals at later ontogenetic stages are better suited to providing accurate growth records (Cullen et al. 2021). The overlap in LAG counts between smaller femora from different localities may reflect different dietary niches occupied by alligators over ontogeny or sexual dimorphism (Gignac et al. 2019). Due to constraints on available prey items small individuals could experience similar growth rates regardless of local climate/environment.

The RWR alligators have low variance in femoral lengths due to their being the same age, but had variable LAG counts. As reported above, the medullary cavity is more variable in the RWR osteohistological thin sections compared to wild samples. Variation in medullary expansion among this population could account for the variation in LAG counts as the medullary cavity erodes earlier LAGs. The formation of an external fundamental system (EFS) at different ages could also affect LAG counts, which suggests a similar variation in LAG counts could exist among wild alligators of the same or very similar ages. Variation in sampling location along the diaphysis could also impact the number of LAGs in the thin section, as the medullary cavity is not the same size along the length of the diaphysis.

Inter-LAG measurements have been demonstrated to be subject to considerable variation and misinterpretation (Cullen et al. 2021). Variation between skeletal elements and in sampling location within the same element have been recognized as sources of variation (Garcia 2011; Cullen et al. 2021). This is particularly pernicious in paleohistological studies where specimen selection is frequently based upon curatorial permission or the fossil record (i.e. taphonomy and collection efforts) (Padian and Lamm 2013; Cullen et al. 2021). Indeed, results indicate that the inter-LAG measurements in *Alligator mississippiensis* appeared to be subject to more variation than simple LAG counts, despite all measurements being taken from one taxon at the same location in the same element. North Carolina alligators particularly had larger average inter-LAG distances, possibly due to the disproportionate number of smaller individuals in that particular sample. One 94mm length Georgia femur had an average inter-LAG distance of 3.38mm, greater than any other thin section in this study. Alligators from North Carolina did have the narrowest inter-LAG distance among the wild individuals included, with one 135mm length femur having mean inter-LAG distance of 0.489mm. In contrast, the Georgia femur with the narrowest average inter-LAG distance, 137mm in length, had and average inter-LAG spacing of 0.952mm. The average inter-LAG distance among Georgia specimens was 0.707mm (SD = 0.375; CoV = 0.53) (Table 7), while among North Carolina alligators the average inter-LAG distance was 0.682mm (SD = 0.373; CoV = 0.55) (Table 8), suggesting elevated rates of bone apposition in Georgia femora. However, an independent T-test did not find any significant difference between the means of these two groups (Table 7), a result unsurprising given the standard deviation of over half the average inter-LAG distance in both cases. These findings emphasize the considerable variation and ambiguous utility of inter-LAG spacing to infer growth rates of individual bones.

Table 8 Scaled mean inter-LAG distance and standard deviation for measured Georgia specimens

ETMNH-Z	Mean Inter-LAG
487	1.250188007
3024	1.594316955
3116	0.98695382
3150	1.181810938
3334	1.114336904
18432	1.745036343
18433	1.045832894
18458	0.952254536
Standard Deviation	***0.610820536***

Table 9 Scaled mean inter-LAG distance and standard deviation for measured North Carolina specimens

ETMNH-Z	Mean Inter-LAG
20007	3.387238983
20009	0.775402415
20010	0.870214976
20011	1.561352876
20012	0.773710372
20013	1.911809935
20014	0.638010718
20015	1.357613228
20016	0.489033813
20017	0.767654495
20020	1.167874947

20021	0.602727273
Standard Deviation	***0.701392568***

Gray Fossil Site *Alligator*

The GFS *Alligator* is an outlier compared to its extant North American relative. The two larger femora retain more LAGs than any extant specimen examined, including fully mature individuals from the Rockefeller Wildlife Refuge (RWR). The smallest GFS femur examined (ETMNH 82: see Figure 10 and Table 6) also has a much higher LAG count compared to similarly sized femora of *A. mississippiensis*. The high LAG count could be due to local environmental conditions causing protracted growth rates, such as lack of appropriate prey or adverse climate conditions, pronounced sexual dimorphism, or endogenously slow growth. Modern *A. mississippiensis* from North Carolina are subject to the shortest growing season and some of the coldest winters of any extant crocodilian, comparable to the Chinese alligator (*Alligator sinensis*) which inhabits slightly lower latitudes and experiences similarly cool winters. The extant North Carolina specimens included in this study experienced a mean annual temperature of 16.08C, similar to that estimated for GFS: 16.8C (Schap et al. 2021) and 16.4C (Riechgelt et al. 2023). Given this similarity in mean temperature between the fossil taxon and extant comparative specimens, a climatic explanation for elevated LAG counts in the GFS *Alligator* may be unlikely.

Food availability, often a function of climatic and abiotic environmental factors, exerts a strong influence on growth rates in crocodilians, including *Alligator* (Webb, 1985; Jacobsen and Kushlan 1989; Thomas Rainwater pers. comm.) which may explain elevated LAG counts in the GFS *Alligator*. As opportunistic generalist predators the diet of an individual alligator varies with ontogeny and local habitats. Smaller *A. mississippiensis* prey mostly upon fish, reptiles, and invertebrates which make up ~70% of the stomach contents (Delany and Abercrombie 1986). Mammals are preyed upon more frequently with increased length or where there are abundant aquatic rodents (Delany and Abercrombie 1986; Wolf et al. 1987). The dwarf tapir *Tapirus polkensis* is the most numerous macrovertebrate taxon at GFS and would have potentially been a significant source of food for alligators. Comparison of femoral length of GFS *Alligator* with mass regression equations from Farlow (2005) predicts that the largest fossil femur (ETMNH 8031; not sectioned for this study) was from an animal 247.3cm (8.11ft) in total length, large enough to prey upon many of the mammals from GFS.

The GFS sinkhole pond also had abundant centrarchid fish (Shay Maden, pers. comm.), a family of fish known to be preyed upon by alligators, though not at high rates (Wolf et al. 1987). The GFS fish are mostly small *Lepomis*. Larger fish typical of *A. mississippiensis* stomach contents (Wolfe et al. 1987) are uncommon in GFS sediments (Shay Maden pers. comm.). However, in some Florida lakes shad fish, similarly sized to *Lepomis*, constitute the majority of vertebrates consumed (Delany et al. 1999). Ample remains of centrarchids in the lacustrine sediments could suggest that these fish were a significant component of the GFS *Alligator* diet, replacing other fish which are commonly eaten by *A. mississippiensis* along the United States' coastal plain.

Unfortunately, evidence of predation by *Alligator* is rare at GFS, so little can be said with certainty regarding their local dietary habits. The only direct evidence of predation by GFS *Alligator* are: 1) the remains of a small musk turtle (*Sternotherus palaeodorus*) with two puncture marks in the carapace consistent with a predation attempt by an alligator (Bourque and Schubert 2015); and 2) "acid etched" juvenile *Alligator* osteoderms and limb elements found in the thoracic cavity of a larger articulated *Alligator* fossil (Shawn Haugrud, pers. comm.). Turtles are abundant in the GFS sediments and are known to make up more than one fifth of the vertebrates in alligator stomachs (Delany and Abercrombie 1986). The paucity of evidence of predation on turtles at GFS may reflect actual dietary habits of the GFS *Alligator* or a lack of recognition or preservation of predated remains. Alligators have powerful stomach acids that may severely affect the ability of bone to withstand the fossilization process after having passed through the digestive tract (Fisher 1981). Alligators are also relatively rare within the GFS sediments (MNI = 7; Haugrud 2023 MS Thesis) so examples of turtle predation may also be rare in the GFS fossil record, even if they were commonly predated upon by the GFS *Alligator*.

Given the abundance of prey items available to GFS *Alligator* across their ontogeny, it seems unlikely that malnourishment is responsible for the elevated femoral LAG counts. Apart from sexual dimorphism (which was not examined in this study) this appears to leave a slow endogenous growth rate as the most likely explanation for the elevated femoral LAG counts in the GFS *Alligator*. Evidence for an endogenously slow femoral growth rate can be seen in the time series data for ETMNH 18124 and ETMNH 7729 (Figures 15-16). Both specimens show an abrupt transition in LAG spacing at LAG 17. After this transition, LAG spacing stops increasing rapidly and appears to plateau. Before LAG 17 both specimens had achieved more than 90% of their growth. In the past this transition may have been interpreted as reaching asymptotic growth, but recent studies have demonstrated that equidistant apposition may actually represent reaching an inflection point in growth (Cullen et al. 2021), such that growth rate is still high but no longer increasing. Regardless of the interpretation (whether the transition represents asymptotic growth or the growth inflection point) it likely means that these two specimens were at least sexually mature (Padian and Lamm 2013). As reported above, the largest femur from the GFS *Alligator* is predicted to belong to an individual with a total length of 247.3cm. Only one fossil humerus is slightly longer than this femur, indicating the largest represented GFS alligators were ~250cm in total length, well below the largest *A. mississippieniss* (>400cm total length) encountered today (Woodward et al. 1995). Other archosaur taxa are known to attain small adult size by maintaining a slow growth rate (Cullen et al. 2020; Qin et al. 2021) and this may be the case for the GFS *Alligator* as well. If the slower growth rate of the GFS *Alligator* is endogenous, this may reflect a continuation into the Pliocene of small adult size, as seen in other continental *Alligator* species earlier in the Cenozoic (Hastings et al. 2023). The osteohistological data presented here provides some evidence that *Alligator mississippiensis* achieved larger adult sizes within its lineage by increasing growth rate during ontogeny, a strategy of increasing adult body size that has been demonstrated in other archosaurs (Cullen et al. 2020; D’emic et al. 2023).

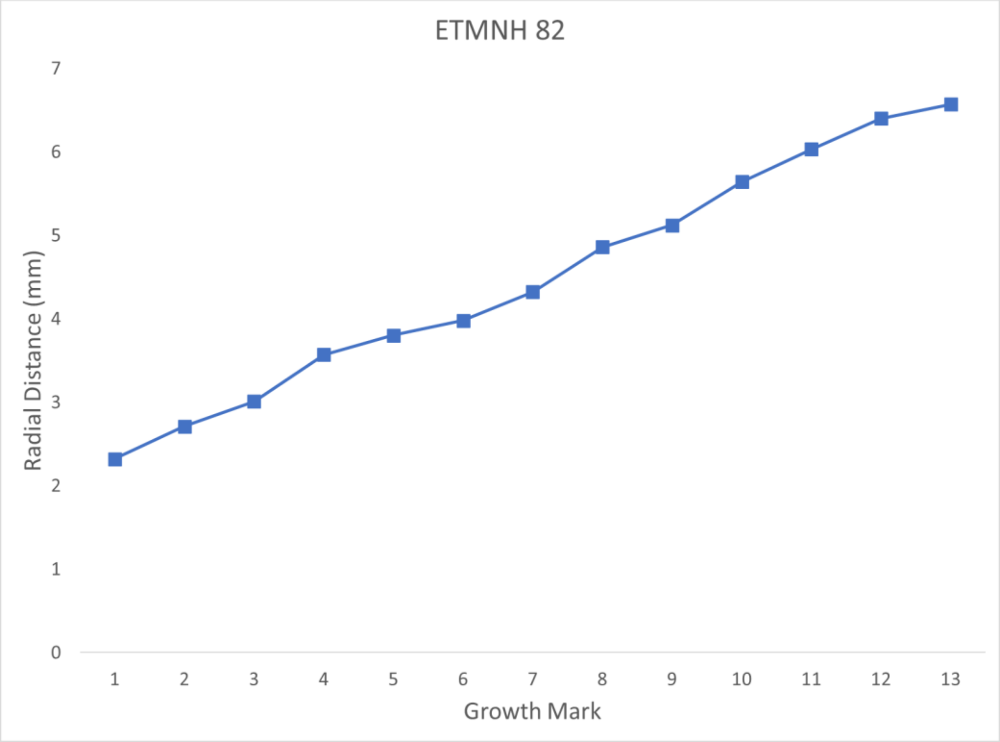

Fig. 10 Increase in radial distance, measured at each LAG in a fossil *Alligator* femur (ETMNH 82) from the Gray Fossil Site.

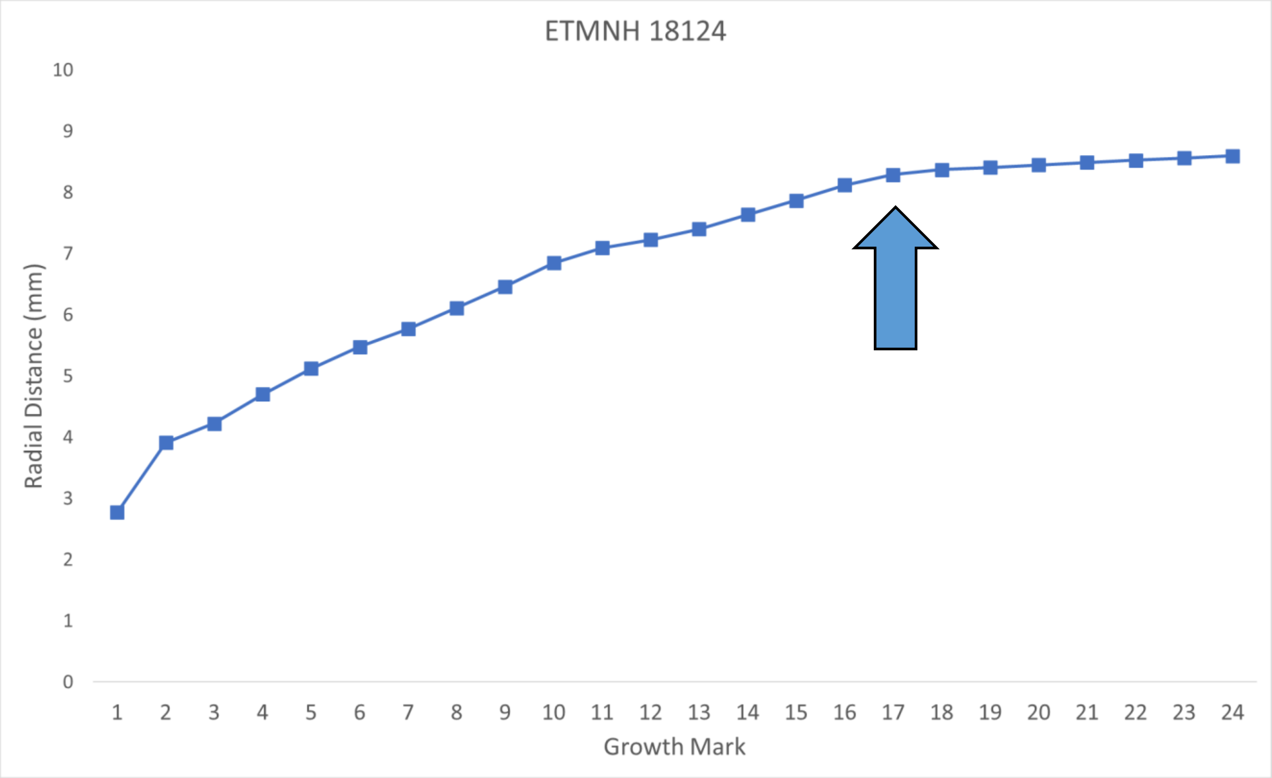

Fig. 11 Increase in radial distance, measured at each LAG in a fossil *Alligator* femur (ETMNH 18124) from the Gray Fossil Site. Arrow indicates transition in LAG spacing.

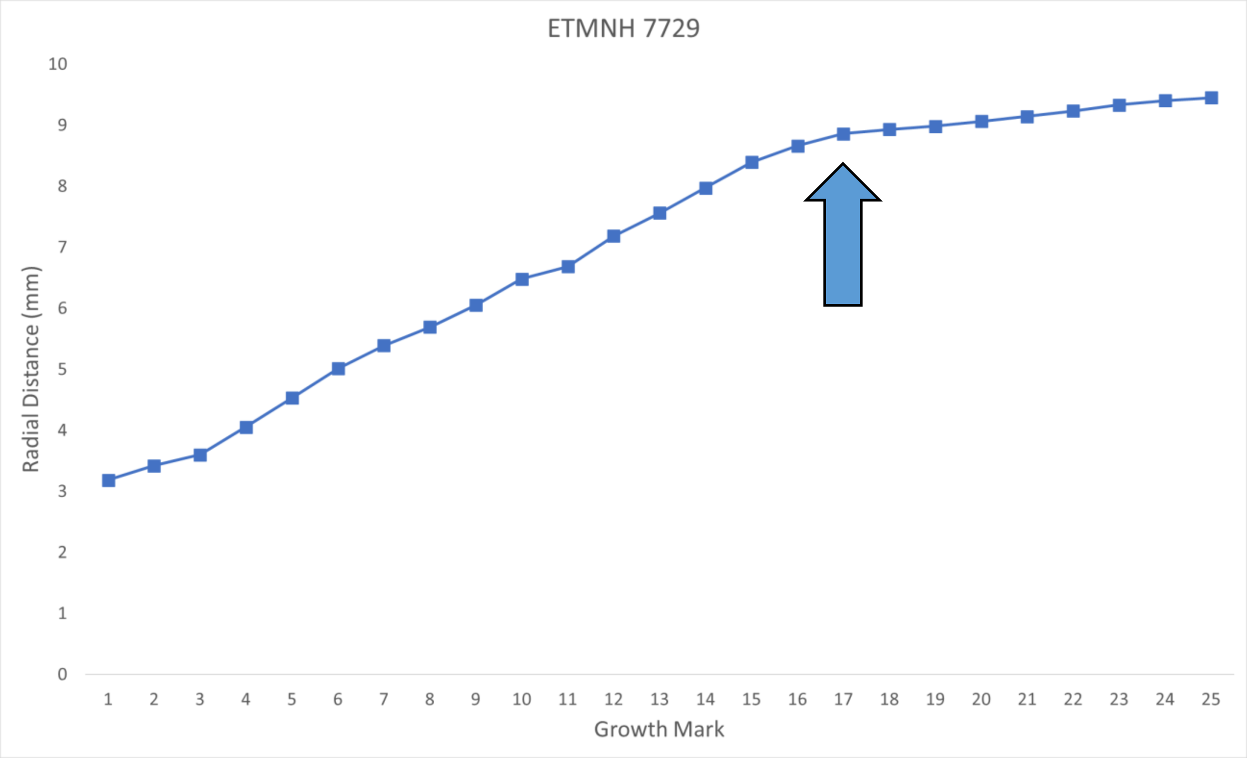

Fig. 12 Increase in radial distance, measured at each LAG in a fossil *Alligator* femur (ETMNH 7729) from the Gray Fossil Site. Arrow indicates transition in LAG spacing.

CHAPTER 5. CONCLUSIONS

- Comparing LAG counts between femora of similar size (thus, experiencing similar ontogenetically determined growth rates at time of death) reveals considerable variation, especially among smaller individuals. However, larger femora do show decreased LAG counts in alligators from Georgia compared to those from cooler climates like the Carolinas and Arkansas.
- LAG spacing (inter-LAG distance) shows more variation than simple comparisons of LAG counts, but also reflect a general trend of increased yearly apposition in Georgia alligators when compared to others. Comparing average LAG spacing shows no statistically significant difference between alligators from different states. This supports other work which suggests comparison of LAG spacing is a poor method of inferring somatic growth rates.
- There is variation in the relationships between the cross-sectional area of the femur, femoral medullary cavity, femoral bone, and femoral length. The total area and bone area of the thin section are strongly linearly correlated, and both are also strongly correlated with femoral length. The correlation between bone area and total area is explained by the fact that they are non-independent values, with bone area calculated from total area by subtracting medullary cavity area. This also means that medullary cavity area scales proportionately to total area similarly across ontogeny. The strong correlation between total area and bone area and femoral length likely reflects biomechanical factors. At larger sizes more bone is needed to support the weight of the alligator. The relationship is nonlinear, reflecting the differential scaling of area (cross section of the femur) and volume (mass of the alligator).
- In comparison to modern *A. mississippiensis* specimens, the Gray Fossil Site *Alligator* shows more femoral LAGs and narrower femoral LAG spacing than any wild *A. mississippiensis*.

This is interpreted as a slower growth rate compared to *Alligator mississippiensis*. Based on the similarity in mean annual temperature between coastal North Carolina and the Gray Fossil Site at the time of deposition, as well as ample prey species preserved within GFS sediments, the slower growth rate and smaller adult body size in the GFS *Alligator* may have been endogenous. Comparison of the GFS *Alligator* with another small *Alligator* species such as *A. sinensis* may help test this hypothesis.

- The captive alligators from Rockefeller Wildlife Refuge (RWR) are also outliers compared to their wild counterparts, in all metrics reported in this study. This is likely to be the result of a rapid growth to asymptotic size and the same (or very similar) age of all RWR specimens compared to wild individuals. Since the RWR alligators included in this study had all formed and EFS, LAG spacing was mostly influenced by the late ontogenetic stage of the specimens, obscuring signals from local geographic and climatic conditions. This underscores the biases that captive animals present in paleohistological inference; more wild animals need to be included in neontological osteohistology.

REFERENCES

Andrade RC, Bantim, RAM, de Lima FJ, dos Santos Campos L, de Souza Eleutério LH, Sayão JM. 2015. New data about the presence and absence of the external fundamental system in archosaurs. Cadernos de Cultura e Ciência. 14(1): 200-211.

Andronowski JM, Crowder C, Soto Martinez M. 2018. Recent advancements in the analysis of bone microstructure: new dimensions in forensic anthropology. Forensic Sciences Research. 3(4): 278–293.

Boardman GS, Schubert BW. 2011. First Mio-Pliocene salamander fossil assemblage from the southern Appalachians. Palaeontologia Electronica. 14(2): 16A.

Bourque JR, Schubert BW. Fossil musk turtles (Kinosternidae, *Sternotherus*) from the late Miocene–early Pliocene (Hemphillian) of Tennessee and Florida. Journal of Vertebrate Paleontology. 35(1): e885441.

Bruder SP, Arnold IC. 1989. Cellular and molecular events during embryonic bone development. Connective tissue research. 20(1-4): 65-71.

Castanet J, Francillon-Vieillot, H, Meunier FJ, Ricqles AD. 1993. Bone and individual aging. In: Hall BK, editor. Bone. Volume 7. Boca Raton: CRC Press. P. 245-283.

Clark GM, Kohl M, Moore HL, Sasowsky ID. 2005. The Gray Fossil Site: A spectacular example in Tennessee of ancient regolith occurrences in carbonate terranes, Valley and Ridge subprovince, southern Appalachians USA. Sinkholes and the Engineering and Environmental Impacts of Karst. 82-90.

Cullen TM., Canale JI, Apesteguía S, Smith ND, Hu D, Makovicky PJ. 2020. Osteohistological analyses reveal diverse strategies of theropod dinosaur body-size evolution. Proceedings of the Royal Society B. 287(1939): 2020-2258.

Cullen, TM, Brown CM, Chiba K, Brink KS, Makovick, PJ, Evans DC. 2021. Growth variability, dimensional scaling, and the interpretation of osteohistological growth data. Biology letters . ; 17(11): 20210383. Available from: https://doi.org/10.1098/rsbl.2021.0383

Currey JD. 2006. Bones: structure and mechanics. Princeton (NJ): Princeton University Press.

de Andrade RCLP, Sena MVA, Araújo EV, Bantim RAM, Riff D, Sayão JM. 2018. Osteohistological study on both fossil and living Caimaninae (Crocodyliformes, Crocodylia) from South America and preliminary comments on growth physiology and ecology. Historical Biology. 32(3): 346-355.

D'Emic, MD, Patrick MO, Riley SS, Ignacio C, Thomas RP, David V, Diego P, Anjali D, Rodolfo AC, and Kristina ACR. 2023. Developmental strategies underlying gigantism and miniaturization in non-avialan theropod dinosaurs. Science. 379(6634): 811-814.

Delany MF, Abercrombie CL. 1986. American alligator food habits in northcentral Florida. The Journal of Wildlife Management. p. 348-353.

Delany MF, Linda SB, Moore CT. 1999. Diet and condition of American alligators in 4 Florida lakes. Proceedings of the Annual Conference of the Southeastern Association of Fish and Wildlife Agencies (53): 375-389.

de Margerie, E, Cubo, J, Castanet J. 2002. Bone typology and growth rate: testing and quantifying ‘Amprino’s rule’in the mallard (*Anas platyrhynchos*). Comptes rendus biologies. 325(3), 221-230.

Farlow JO, Hurlburt GR, Elsey RM, Britton AR, Langston Jr W. 2005. Femoral dimensions and body size of *Alligator mississippiensis*: estimating the size of extinct mesoeucrocodylians. Journal of Vertebrate Paleontology. 25(2): 354-369.

Fisher DC. 1981. Crocodilian scatology, microvertebrate concentrations, and enamel-less teeth. Paleobiology. 7(2): 262-275.

Garcia BJ. 2011. Skeletochronology of the American Alligator (*Alligator mississippiensis*): Examination of the Utility of Elements for Histological Study [master's thesis]. [Tallahassee (FL)]: Florida State University.

Gignac PM, O'Brien HD, Turner AH, Erickson GM. 2019. Feeding in crocodylians and their relatives: functional insights from ontogeny and evolution. Feeding in Vertebrates: Evolution, Morphology, Behavior, Biomechanics. p. 575-610.

Hastings AK, Schubert BW, Bourque JR, Hulbert Jr, RC. 2023. Oldest record of *Alligator* in southeastern North America. Palaeontologia Electronica. 26(1): 1-19.

Heck CT, Holly NW. 2021. Intraskeletal bone growth patterns in the North Island Brown Kiwi (*Apteryx mantelli*): Growth mark discrepancy and implications for extinct taxa. Journal of Anatomy. 239(5): 1075-1095.

Hinrichs J. 2016. Are lines of arrested growth in bone indicative of seasonal metabolic suppression in bears? [master's thesis]. [Fort Collins (CO)]: Colorado State University.

Horner JR, Padian K, de Ricqlès A. 2001. Comparative osteohistology of some embryonic and perinatal archosaurs: developmental and behavioral implications for dinosaurs. Paleobiology. 27(1): 39-58.

Hutton JM. 1986. Age determination of living Nile crocodiles from the cortical stratification of bone. Copeia. 1986(2):332–341.

Jacobsen T, Kushlan JA. 1989. Growth dynamics in the American alligator (*Alligator mississippiensis*). Journal of Zoology. 219(2): 309-328.

Ikejiri T. 2012. Histology-based morphology of the neurocentral synchondrosis in *Alligator mississippiensis* (Archosauria, Crocodylia). Anatomical Record. 295(1): 18–31.

Klein N, Torsten S, Thomas T. 2009. Skeletochronology and isotopic analysis of a captive individual of *Alligator mississippiensis* Daudin, 1802. Fossil Record. 12(2): 121-131**.**

Klevezal GA. 1996. Recording structures of mammals: determination of age and reconstruction of life history. Rotterdam (NL): A. A. Balkema.

Köhler M, Marín-Moratalla N, Jordana X, Aanes R. 2012. Seasonal bone growth and physiology in endotherms shed light on dinosaur physiology. Nature. 487(7407): 358-361.

Kolb C, Torsten S, Kristof V, Analia MF, Eli A, Alexandra AEVG, Lars WVHO, Shoji H, Marcelo RSV. 2015. Mammalian bone palaeohistology: a survey and new data with emphasis on island forms. PeerJ; e1358.

Lance VA. 2003. Alligator physiology and life history: the importance of temperature. Experimental gerontology. 38(7): 801-805.

Lieberman DE, Polk JD, Demes B. 2004. Predicting long bone loading from cross-sectional geometry. American Journal of Physical Anthropology: The Official Publication of the American Association of Physical Anthropologists. 123(2): 156-171.

Liu YSC, Jacques FM. 2010. *Sinomenium macrocarpum* sp. nov. (Menispermaceae) from the Miocene–Pliocene transition of Gray, northeast Tennessee, USA. Review of Palaeobotany and Palynology. 159(1-2): 112-122.

Mead JI, Schubert BW, Wallace SC, Swift SL. 2012. Helodermatid lizard from the Mio-Pliocene oak-hickory forest of Tennessee, eastern USA, and a review of monstersaurian osteoderms. Acta Palaeontologica Polonica. 57(1): 111-121.

Nickum MJ, Masser M, Reigh R, Nickum JG. 2018. Alligator (Alligator mississippiensis) aquaculture in the United States. Reviews in Fisheries Science & Aquaculture. 26(1): 86-98.

Whitelaw JL, Mickus K, Whitelaw MJ, Nave J. 2008. High-resolution gravity study of the Gray Fossil Site. Geophysics 73(2): 25-32.

Murphy TM. 1977. Distribution, movement and population dynamics of the American alligator in a thermally altered reservoir [master's thesis]. [Athens (GA)]: University of Georgia, Athens.

Padian K, Lamm ET. 2013. Bone Histology of Fossil Tetrapods: Advancing Methods, Analysis, and Interpretation. 1st edition. Berkeley (CA): University of California Press.

Petermann, H, Sander M. 2013. Histological evidence for muscle insertion in extant amniote femora: implications for muscle reconstruction in fossils. Journal of Anatomy. 222(4): 419-436.

Qin Z, Zhao Q, Choiniere JN, Clark JM, Benton MJ, Xu X. 2021. Growth and miniaturization among alvarezsauroid dinosaurs. Current Biology. 31(16): 3687-3693.

Rainwater TR, Woodward HN, Woodward AR, Wilkinson PM. 2021. Evidence of determinate growth in an American alligator (*Alligator mississippiensis*) based on long-term recapture and osteohistological confirmation. Anatomical Record. 305(10): 3101-3108.

Reichgelt T, Baumgartner A, Feng R, Willard DA. 2023. Poleward amplification, seasonal rainfall and forest heterogeneity in the Miocene of the eastern USA. Global and Planetary Change; 222: 104073. Available from: https://doi.org/10.1016/j.gloplacha.2023.104073

de Ricqlès AJ. 1976. On bone histology of fossil and living reptiles, with comments on its functional and evolutionary significance. In: Bellairs A, Cox CB, editors. Morphology and Biology of Reptiles. New York, (NY): Academic Press. p. 123-151. (Linnean Society Symposium Series; number 3)

Samuels JX, Bredehoeft KE, Wallace SC. 2018. A new species of *Gulo* from the Early Pliocene Gray Fossil Site (Eastern United States); rethinking the evolution of wolverines. PeerJ; 6: e4648. Available from: https://doi.org/10.7717/peerj.4648

Samuels JX, Schap J. Early Pliocene leporids from the Gray Fossil Site of Tennessee. Eastern Paleontologist. 2021(8): 1-23.

Schap JA, Samuels JX, Joyner TA. 2021. Ecometric estimation of present and past climate of North America using crown heights of rodents and lagomorphs. Palaeogeography, Palaeoclimatology, Palaeoecology. 562: 110-144.

Schweitzer MH, Elsey RM, Dacke CG, Horner JR, Lamm E-T. 2007. Do egg-laying crocodilian (Alligator mississippiensis) archosaurs form medullary bone? Bone. 2007(40): 1152–1158.

Seebacher F, Elsey RM, Trosclair PL. 2003. Body temperature null distributions in reptiles with nonzero heat capacity: Seasonal thermoregulation in the American alligator (*Alligator mississippiensis*). Physiological and Biochemical Zoology. 76(3): 348–359.

Shine TS, Bohme W, Nickel H, Thies DF, Wilms T. 2001. Rediscovery of relict populations of the Nile crocodile *Crocodylus niloticus* in south-eastern Mauritania, with observations on their natural history. Oxyx. 35(3): 260–262.

Shunk AJ, Driese SG, Clark GM. 2006. Latest Miocene to earliest Pliocene sedimentation and climate record derived from paleosinkhole fill deposits, Gray Fossil Site, northeastern Tennessee, USA. Palaeogeography, Palaeoclimatology, Palaeoecology. 231(3-4): 265-278.

Shunk AJ, Driese SG, Dunbar JA. 2009. Late Tertiary paleoclimatic interpretation from lacustrine rhythmites in the Gray Fossil Site, northeastern Tennessee, USA. Journal of Paleolimnology. 42: 11-24.

Sims NA, Jonathan HG. 2008. Bone remodeling: Multiple cellular interactions required for coupling of bone formation and resorption. Seminars in cell & developmental biology. 19(5): 444-451.

Smith MM, Hall BK. 1990. Development and evolutionary origins of vertebrate skeletogenic and odontogenic tissues. Biological Reviews. 65(3): 277-373.

Tucker AD. 1997. Validation of skeletochronology to determine age of freshwater crocodiles (*Crocodylus johnstoni*). Aust J Mar Freshw Res. 48(4):343–351.

Tumarkin-Deratzian AR, Vann DR, Dodson P. 2007. Growth and textural ageing in long bones of the American alligator *Alligator mississippiensis*. Zoological Journal of the Linnean Society. 150(1): 1-39.

Wallace SC, Wang X. 2004. Two new carnivores from an unusual late Tertiary forest biota in eastern North America. Nature. 431(7008): 556-559.

Webb JGW. 1985. Survey of a pristine population of freshwater crocodiles in the Liverpool River, Arnhem Land, Australia. National Geographic Society Research Report. 1979: 841–852.

Wolfe JL, Bradshaw DK, Chabreck RH. 1987. Alligator feeding habits: new data and a review. Gulf of Mexico Science, 9(1): 1.

Woodward AR, White JH, Linda SB. 1995. Maximum size of the alligator (*Alligator mississippiensis*). Journal of Herpetology. p. 507-513.

Woodward HN, Horner JR, Farlow JO. 2011. Osteohistological evidence for determinate growth in the American alligator. Journal of Herpetology. 45(3): 339–342.

Woodward HN, Horner JR, Farlow JO. 2014. Quantification of intraskeletal histovariability in *Alligator mississippiensis* and implications for vertebrate osteohistology. PeerJ. 2014(1): 1–34.

Woodward HN. 2019. *Maiasaura* (Dinosauria: Hadrosauridae) tibia osteohistology reveals non-annual cortical vascular rings in young of the year. Frontiers in Earth Science; 7(50). Available from: https://doi.org/10.3389/feart.2019.00050

Worobiec E, Liu YSC, Zavada MS. 2013. Palaeoenvironment of late Neogene lacustrine sediments at the Gray Fossil Site, Tennessee, USA. Annales Societatis Geologorum Poloniae. 83(1): 51-63.

Zobaa MK, Zavada MS, Whitelaw MJ, Shunk AJ, Oboh-Ikuenobe FE. 2011. Palynology and palynofacies analyses of the Gray Fossil Site, eastern Tennessee: their role in understanding the basin-fill history. Palaeogeography, Palaeoclimatology, Palaeoecology. 308(3-4): 433-444.

VITA

R. DAVIS GUNNIN

Education:	B.S. Geosciences (Paleontology), East Tennessee State University, Johnson City, Tennessee, 2021
	Public Schools, Johnson City, Tennessee
Professional Experience:	Lab Assistant, Gray Fossil Site, Gray, Tennessee, 2018
	Collections Assistant, Gray Fossil Site, Gray, Tennessee, 2019 – 2023
	Teaching Assistant, East Tennessee State University, Johnson City, Tennessee, 2021-2023
Honors and Awards:	Best New Paleontology Undergraduate Student, East Tennessee State University, 2018
	1st Place Undergraduate Biological Sciences Poster Presentation, Appalachian Student Research Forum, 2019
	Best Undergraduate Student in Paleontology, East Tennessee State University, 2021
	Collins Chew Research Award, East Tennessee State University, 2023
	Travis Durham Memorial Scholarship, East Tennessee State University, 2023